Supporting Information

Fluorination on cyclopentadithiophene-based hole-transport material for high-performance perovskite solar cells

Gizachew Belay Adugna,‡[a,b] Kun-Mu Lee,‡*[c,d,e,f] Hsiao-Chi Hsieh,*[g] Shih- I Lu,*[a] Yu-Chien Hsieh,[a] June Hung Yang,[a] Wei-Hao Chiu,[c,e] Kang-Ling Liau,[h] Yu-Tai Tao[b] and Yan-Duo Lin*[a]

[a]Department of Chemistry, Soochow University, Taipei 11102, Taiwan
[b]Institute of Chemistry, Academia Sinica, Taipei 115024, Taiwan
[c]Department of Chemical and Materials Engineering, Chang Gung University, Taoyuan 33302, Taiwan
[d]Division of Neonatology, Department of Pediatrics, Chang Gung Memorial Hospital, Linkou Taoyuan 33305, Taiwan
[e]Center for Sustainability and Energy Technologies, Chang Gung University, Taoyuan 33302, Taiwan
[f]College of Environment and Resources, Ming Chi University of Technology, New Taipei City, 24301, Taiwan
[g]Department of Applied Materials Science and Technology, Minghsin University of Science and Technology, Hsinchu, Taiwan
[h]Department of Chemistry, National Central University, Taoyuan 32001, Taiwan

‡ These authors contributed equally to this work.

Email: ydlin@scu.edu.tw

Materials and Reagents

All solvents and chemicals were purchased from Aldrich, with the purity more than 98%. The thin-layer chromatography (TLC) was conducted with Merck KGaA precoated TLC Silica gel 60F254 on aluminum sheets. Flash column chromatography was performed on glass columns packed with silica gel using Silicycle UltraPure SilicaFlash P60, 40−63 mm (230−400 mesh). Unless otherwise specified, all reactions and manipulations were carried out under a nitrogen atmosphere. Solvents of reagent grade were used for syntheses and those of spectroscopy grade for spectra measurements. Solvents were dried by standard procedures. Compounds **1**, **2**, **3**, **4**, **5**, **6**, **7**, and **8** have been previously reported. [1,2]

Characterization

^{1}H and ^{13}C NMR spectra were recorded on a Bruker 500 MHz spectrometer. Fast atom bombardment (FAB) mass spectra were recorded on a Jeol JMS 700 double-focusing spectrometer. UV spectra were measured on a Jasco V-530 double beam spectrophotometer. Fluorescence spectra were recorded on a Hitachi F-4500 fluorescence spectrophotometer. Cyclic voltammetry experiments were performed with a CHI-621A electrochemical analyzer. All measurements were carried out at room temperature with a conventional three-electrode configuration that consisted of a platinum working electrode, an auxiliary electrode, and a non-aqueous $Ag/AgNO_3$ reference electrode. The SEM images were obtained by using a field-emission scanning electron microscope (JEOL-7401). A Nano-Scope NS3A system (Digital Instrument) was used to obtain the AFM images of the surface morphologies and thicknesses of various thin films. X-ray photoelectron spectroscopy (XPS) was collected with a VG ESCA Scientific Theta Probe system with a monochromatic Al Kα source (1486.6 eV) operated under ultra-high vacuum ($< 2.5 \times 10^{-10}$ Torr) and analyzed by XPSPEAKS41 software. In addition, charge neutralization was used during all measurements. All binding energy were calibrated by shifting the C 1s peak to 284.8 eV.

Solar cell fabrication.

A tin oxide aqueous solution with a weight percentage of 3% was spin-coated onto the substrate at 3500 rpm for 30 seconds to form the SnO_2 electron transfer layer. This layer was then annealed at 150°C for 40 minutes and cooled to room temperature. After cooling to room temperature, the substrate was transferred to a nitrogen-filled glove box. Then, the perovskite ($Cs_{0.05}MA_{0.2}FA_{0.75}Pb(Br_{0.05}I_{0.95})_3$) layer was prepared using a single-step method. The mixture of 576.3 mg of PbI_2 (99.9985%, Alfa Aesar, Harverhill, MA, USA), 161.2 mg of formamidinium iodide (FAI, 99.99%, FMPV®, FrontMaterials Co. Ltd., Taipei, Taiwan), 14 mg of methylammonium bromide (MABr, ECHO chemical, Miaoli, Taiwan), 16.2 mg of Cesium iodide (CsI, Aldrich, Burlington, VT, USA) and 19.8 mg of methylammonium iodide (CH_3NH_3I, MAI, > 98%, STAREK®, Starek Scientific Co. Ltd., Taipei, Taiwan) dissolved in 0.8 mL dimethylformamide (DMF, Tedia, OH, USA) and 0.2 mL Dimethyl sulfoxide (DMSO, 99%, Echo Chemical Co., Ltd., Miaoli, Taiwan) was stirred at 60 ˚C for 8 h and was coated onto the TiO_2 substrate by a two-step spin-coating process at 1000 and 5000 rpm for 10 and 20 sec, respectively. At the second spin-coating step, the substrate/films were treated with 75 µL toluene by drop-casting. The substrate was dried at 100 °C on a hot plate for 10 min. The **YC** molecules studied in this work were dissolved in chlorobenzene (40 mg/mL) and spin-coated on the substrate at 2000 rpm for 30 s. The solution of spiro-OMeTAD was prepared in chlorobenzene (40 mg/mL) and mixed with 17.5 µL solution of lithium bis-trifluoromethanesulfonimide (Li-TSFI, 520 mg in 1 mL acetonitrile) and 28.5 µL 4-*tert*-butylpyridine. The solution was spin-coated on substrate at 2000 rpm for 30 s. Finally, the Ag counter electrode (~100 nm) was deposited by thermal evaporation. The active area of the electrode was fixed at 0.16 cm^2. *J-V* curves were recorded with a Keithley 2400 source meter under simulated AM 1.5G sunlight, calibrated to 100 mW/cm^2. The reported device characteristics were estimated from the measured *J-V* curves.

Solar cell performance measurement

Solar cell efficiencies were evaluated under simulated one sun irradiation from a Xe arc lamp with an AM 1.5 global filter. Irradiance was characterized using a calibrated spectrometer and illumination intensity was set using an NREL certified silicon diode with an integrated KG1 optical filter. Spectral mismatch factors were calculated for each device in this report to be less than 5%. IPCE spectra were measured in air using a commercial IPCE set-up (Enlitech, QE-R).

Mobility measurements

In order to assess the potential of **YC-oF**, **YC-mF**, **YC-H** and spiro-OMeTAD as hole-transport materials, hole-only devices were fabricated with the device structure of ITO/PEDOT:PSS/HTM/Al. Hole mobilities were calculated by the space-charge-limited current (SCLC) method using the Mott–Gurney law, by fitting experimental data to equation (1) in the voltage range where the obtained slope in the double log plot is equal to 2.

$$J = \frac{9}{8}\varepsilon_r\varepsilon_0\mu_h\frac{V^2}{d^3} \quad (1)$$

In equation (1), J is the current density, ε_0 is the permittivity of free space (8.85 x10^{-12} F m^{-1}), ε_r is the relative permittivity of the material (approaching 3 for organic semiconductors), μ_h is the hole mobility, V is the applied voltage and d is the thickness of the active layer.

The hole-only devices were fabricated by spin-coating PEDOT:PSS (Clevios P, VP Al4083) onto pre-cleaned, patterned indium tin oxide (ITO) substrates (15 Ω/square) (Kintec). A film of the HTM was spin-coated on top from chloroform solution with a concentration of 40 mg mL^{-1}. The film thickness was varied by using different spin-coating speeds. As a counter electrode, Al was deposited on top by vacuum evaporation. The current density–voltage curves of the devices were recorded with

a Keithley 2400 Source meter.

Computation method

Ground-state geometries and the corresponding vertical excitation energies of the **YC-oF**, **YC-mF** and **YC-H** molecules in THF solution were studied computationally by performing APFD [4] and TD-APFD calculations, respectively, with the 6-31G(d,p) basis set via Gaussian 16 software package [5]. The solvent effect was considered by the polarizable continuum model (PCM) [6]. To further study the interaction between perovskite and **YC** molecules, we conducted geometry optimization within the context of periodic boundary conditions (PBC) in which one molecule of **YC-oF**, **YC-mF** and **YC-H** was placed over the perovskite surface of 4x4x2 cell. The density functional based tight binding method using the GFN1-xTB [7] parametrization of the extended tight-binding (xTB) model Hamiltonian was employed. We used the DFTB engine [8] implemented in the Amsterdam Modeling Suite (AMS) 2022 [9] to perform the calculations.

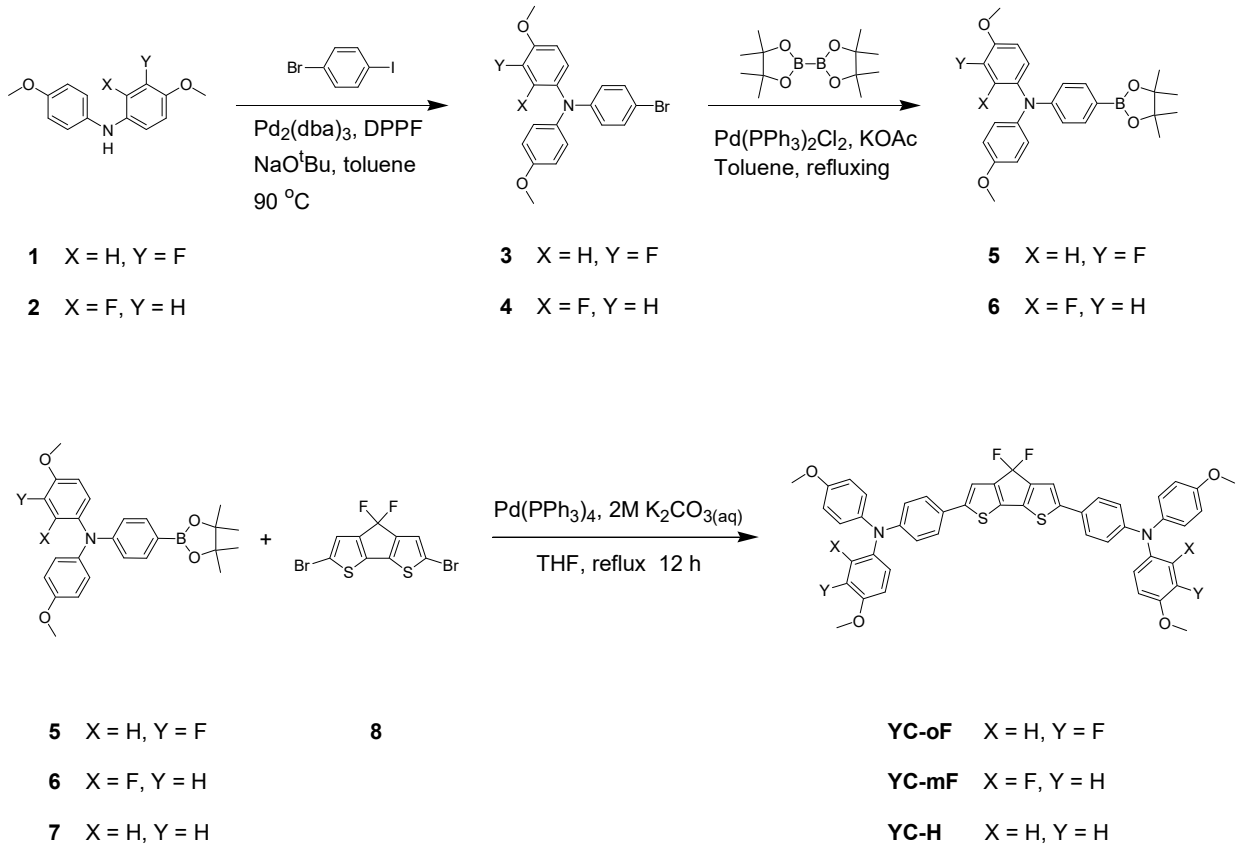

1 X = H, Y = F

2 X = F, Y = H

3 X = H, Y = F

4 X = F, Y = H

5 X = H, Y = F

6 X = F, Y = H

5 X = H, Y = F

6 X = F, Y = H

7 X = H, Y = H

8

YC-oF X = H, Y = F

YC-mF X = F, Y = H

YC-H X = H, Y = H

Scheme S1. Synthetic procedures for **YC-oF**, **YC-mF**, and **YC-H**.

*Synthesis of **YC-oF**:* A heterogeneous mixture of 2 M K_2CO_3 (2 mL), THF (3 mL), **8** (0.18 g, 0.48 mmol), **5** (0.5 g, 1.11 mmol), and $Pd(PPh_3)_4$ (0.036 g, 8 mol %) under argon was heated at 80 °C for 12 h. The mixture was extracted with CH_2Cl_2. The organic layer was separated and dried over anhydrous $MgSO_4$. Evaporation of the solvent gave a crude product, which was purified by silica gel column chromatography using CH_2Cl_2/hexane (1/1) as eluent to afford the desired product as a red solid in 78% yield. mp 135-136 °C; ^{1}H NMR (500 MHz, $CDCl_3$): δ 7.32 (d, J = 8.5, 4H), 7.-15-7.09 (m, 8H), 6.84 (d, J = 8.5, 4H), 6.77 (d, J = 8.5, 4H), 6.70-6.66 (m, 4H), 3.79 (s, 6H), 3.79 (s, 6H) ppm; ^{13}C NMR (125 MHz, $CDCl_3$): δ 160.41, 158.80, 158.72, 158.42, 156.63, 148.44, 147.59, 145.21, 145.00, 144.78, 139.57, 138.12, 138.07, 130.62, 130.60, 126.88, 126.79, 126.59, 126.29, 125.86, 118.27, 115.64, 114.95, 110.96, 110.94, 103.40, 103.22, 55.95, 55.69 ppm.; ^{19}F NMR (376 MHz, DMSO-d6): δ -117.41

(s, 2F), -120.52 (s, 2F). HRMS (FAB) *m/z* [M+1$^+$] calcd for $C_{49}H_{36}F_4N_2O_4S_2$: 856.2053; found: 856.2044.

Synthesis of ***YC-mF***: **YC-mF** was synthesized according to the same procedure as that of **YC-oF**. The product was obtained in 76% yield. mp 132-134 °C; ^{1}H NMR (500 MHz, $CDCl_3$): δ 7.34 (d, J = 8.5, 4H), 7.15 (s, 2H), 7.04 (d, J = 8.5, 4H), 6.92 (d, J = 8.5, 4H), 6.86-6.80 (m, 10H), 3.86 (s, 6H), 3.79 (s, 6H) ppm; ^{13}C NMR (125 MHz, $CDCl_3$): δ 156.76, 153.88, 151.92, 148.19, 147.38, 145.36, 145.14, 144.92, 144.04, 143.96, 141.24, 141.18, 140.11, 138.37, 127.38, 126.96, 126.32, 121.41, 120.27, 120.25, 115.97, 115.15, 114.42, 113.24, 113.08, 56.89, 55.71 ppm.; ^{19}F NMR (376 MHz, DMSO-d6): δ -120.51 (s, 2F), -132.75 (s, 2F). HRMS (FAB) *m/z* [M+1$^+$] calcd for $C_{49}H_{36}F_4N_2O_4S_2$: 856.2053; found: 856.2048.

Synthesis of ***YC-H***: **YC-H** was synthesized according to the same procedure as that of **YC-oF**. The product was obtained in 71% yield. mp 132-134 °C; ^{1}H NMR (500 MHz, $CDCl_3$): δ 7.32 (d, J = 8.5, 4H), 7.13 (s, 2H), 7.06 (d, J = 8.5, 8H), 6.88 (d, J = 8.5, 4H), 6.83 (d, J = 8.5, 8H), 3.78 (s, 12H) ppm; ^{13}C NMR (125 MHz, $CDCl_3$): δ 156.39, 148.85, 147.57, 145.05, 144.83, 140.61, 138.15, 127.06, 126.23, 120.38, 115.68, 115.00, 55.71 ppm.; ^{19}F NMR (376 MHz, DMSO-d6): δ -120.51 (s, 2F); HRMS (FAB) *m/z* [M+1$^+$] calcd for $C_{49}H_{38}F_2N_2O_4S_2$: 820.2241; found: 820.2248.

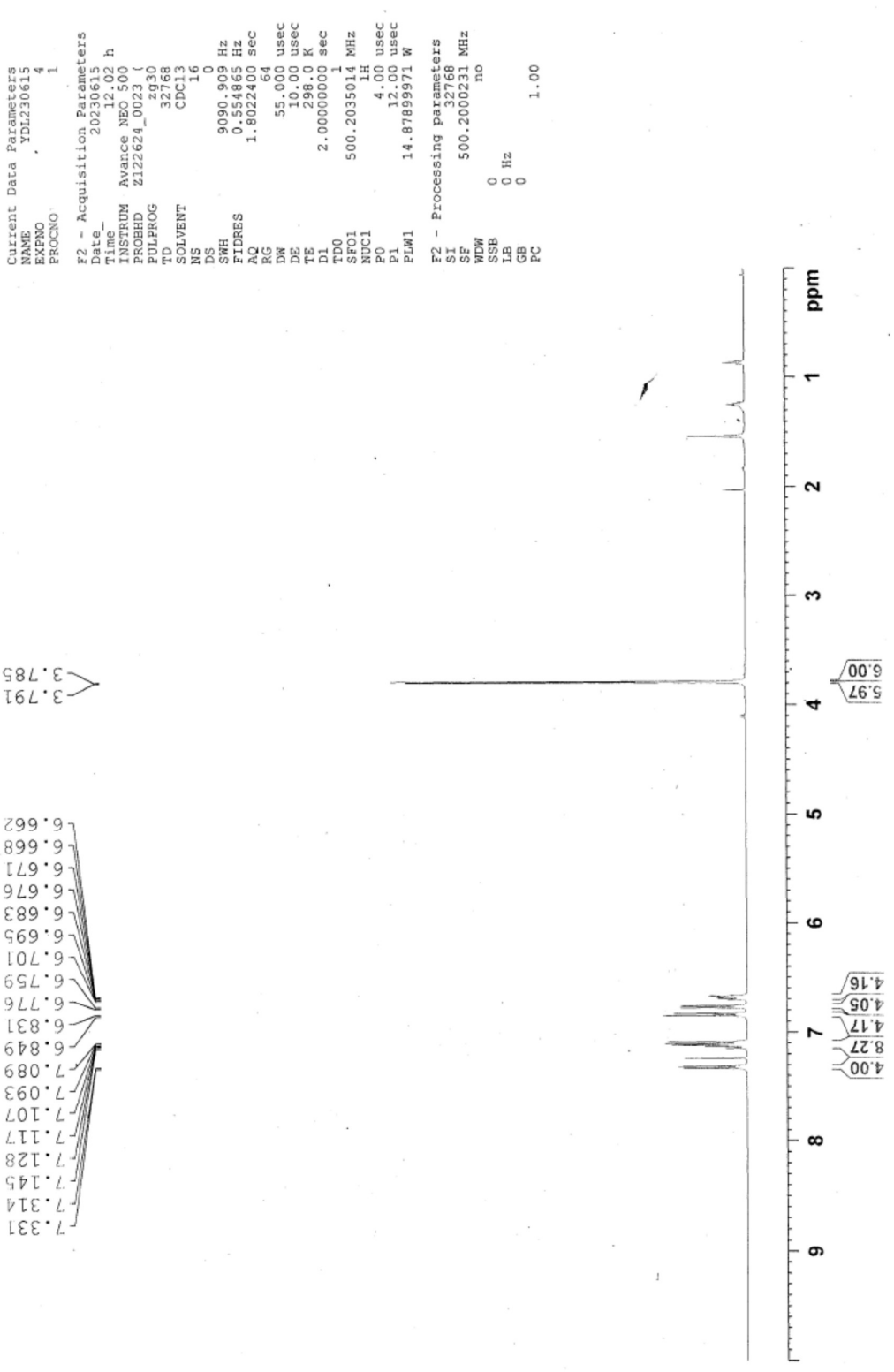

Figure S1. ^{1}H NMR spectrum of compound **YC-oF**.

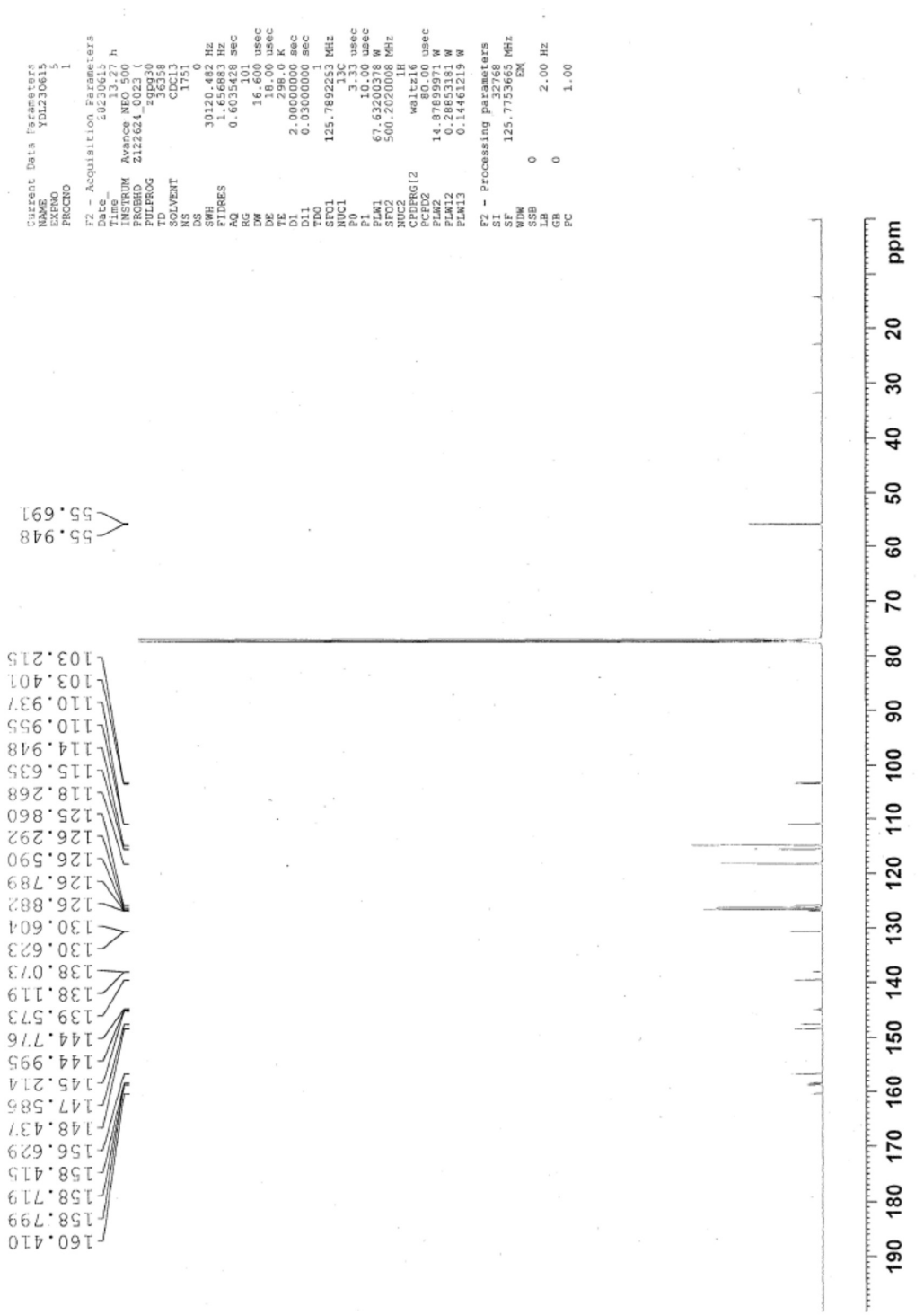

Figure S2. ^{13}C NMR spectrum of compound **YC-oF**.

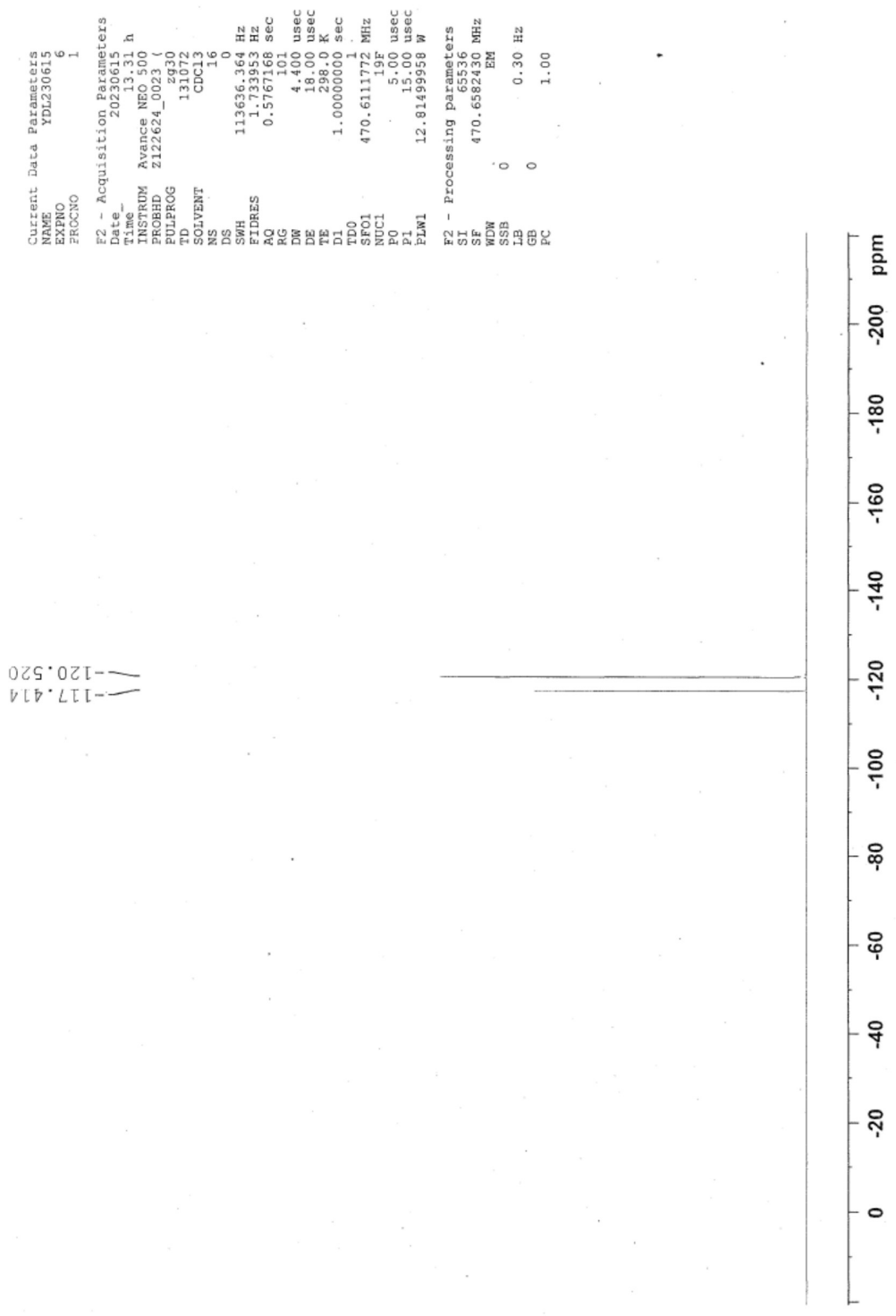

Figure S3. ^{19}F NMR spectrum of compound **YC-oF**.

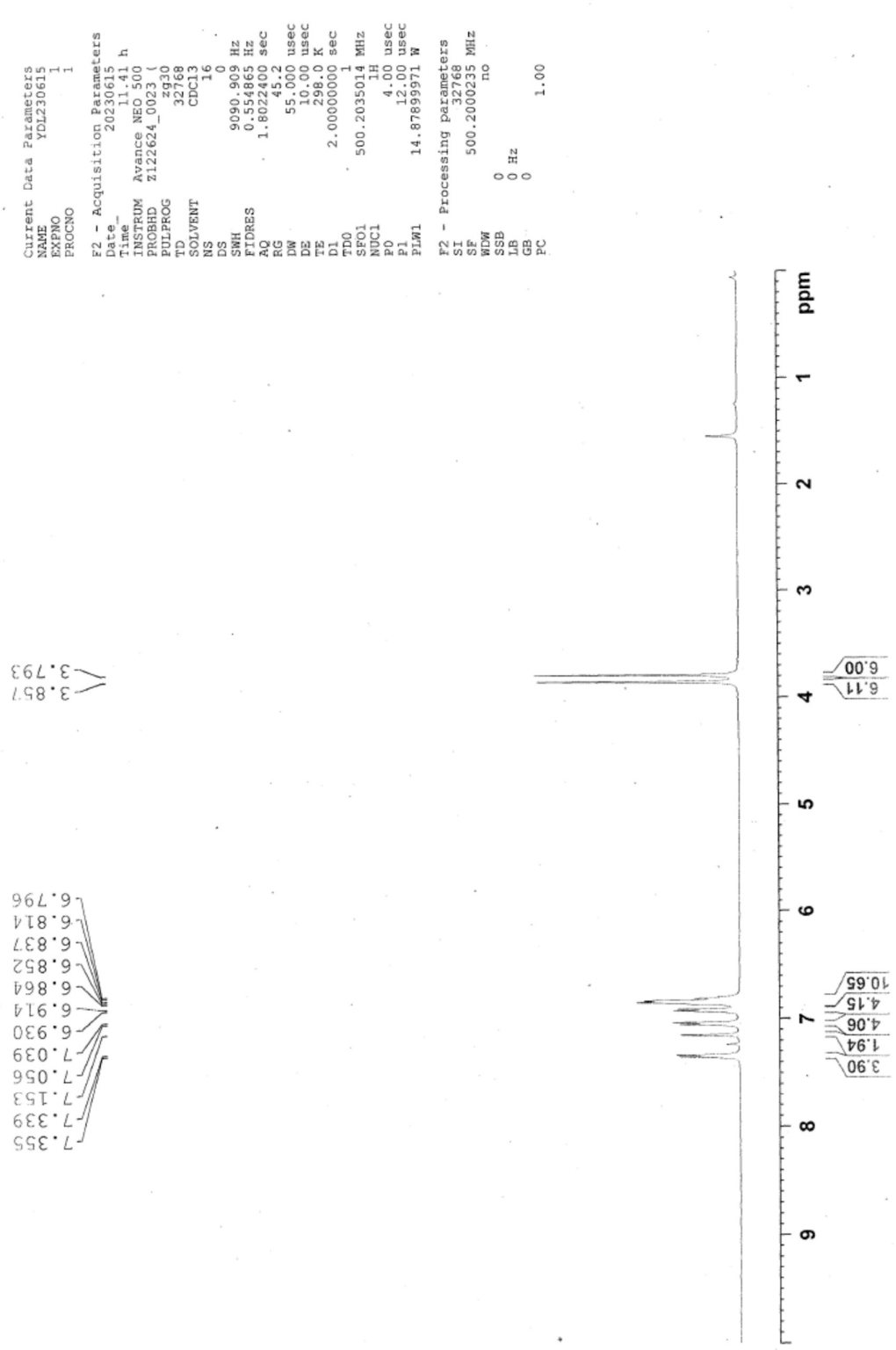

Figure S4. ^{1}H NMR spectrum of compound **YC-mF**.

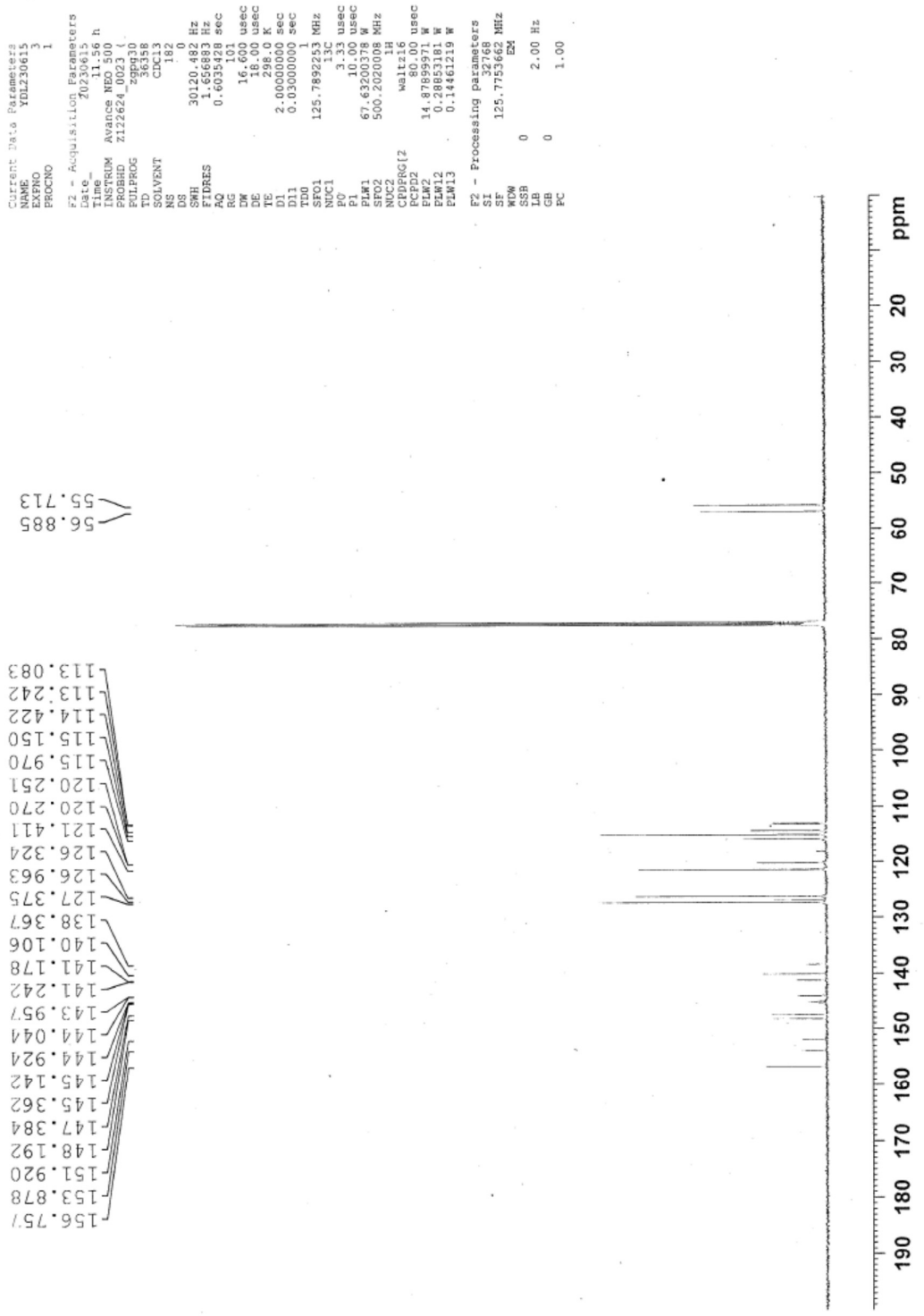

Figure S5. ^{13}C NMR spectrum of compound **YC-mF**.

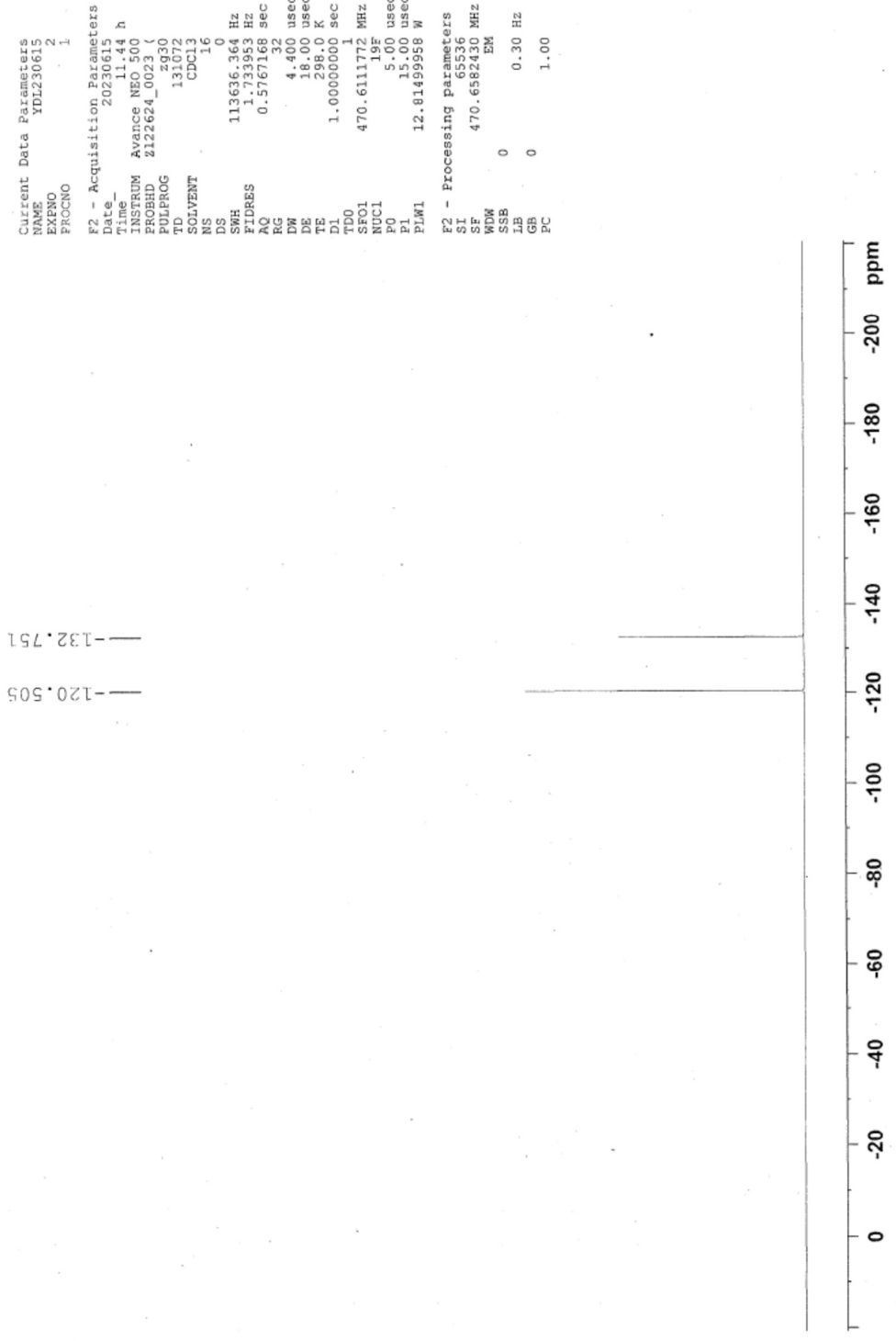

Figure S6. ^{19}F NMR spectrum of compound **YC-mF**.

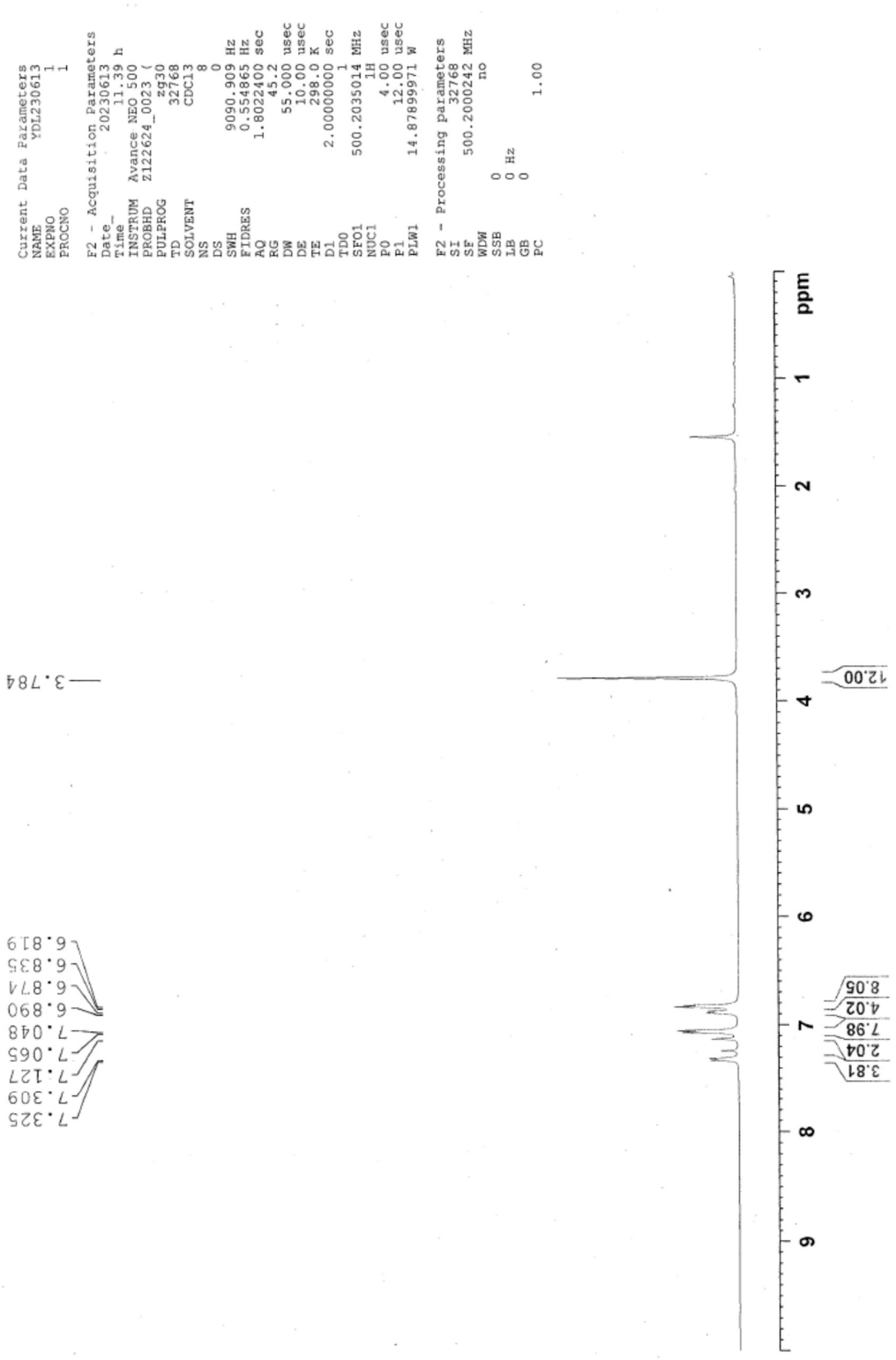

Figure S7. ^{1}H NMR spectrum of compound **YC-H**.

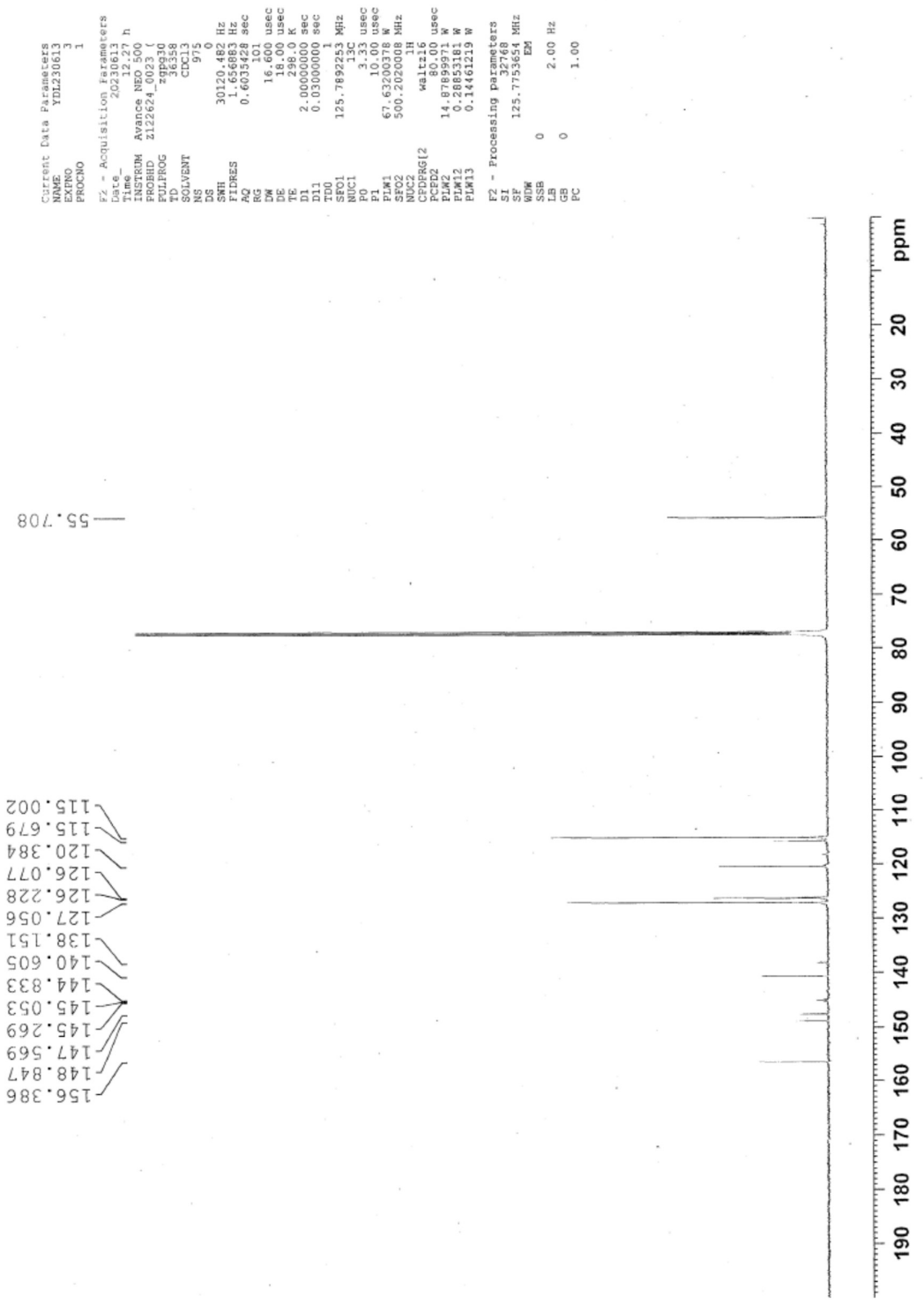

Figure S8. ^{13}C NMR spectrum of compound **YC-H**.

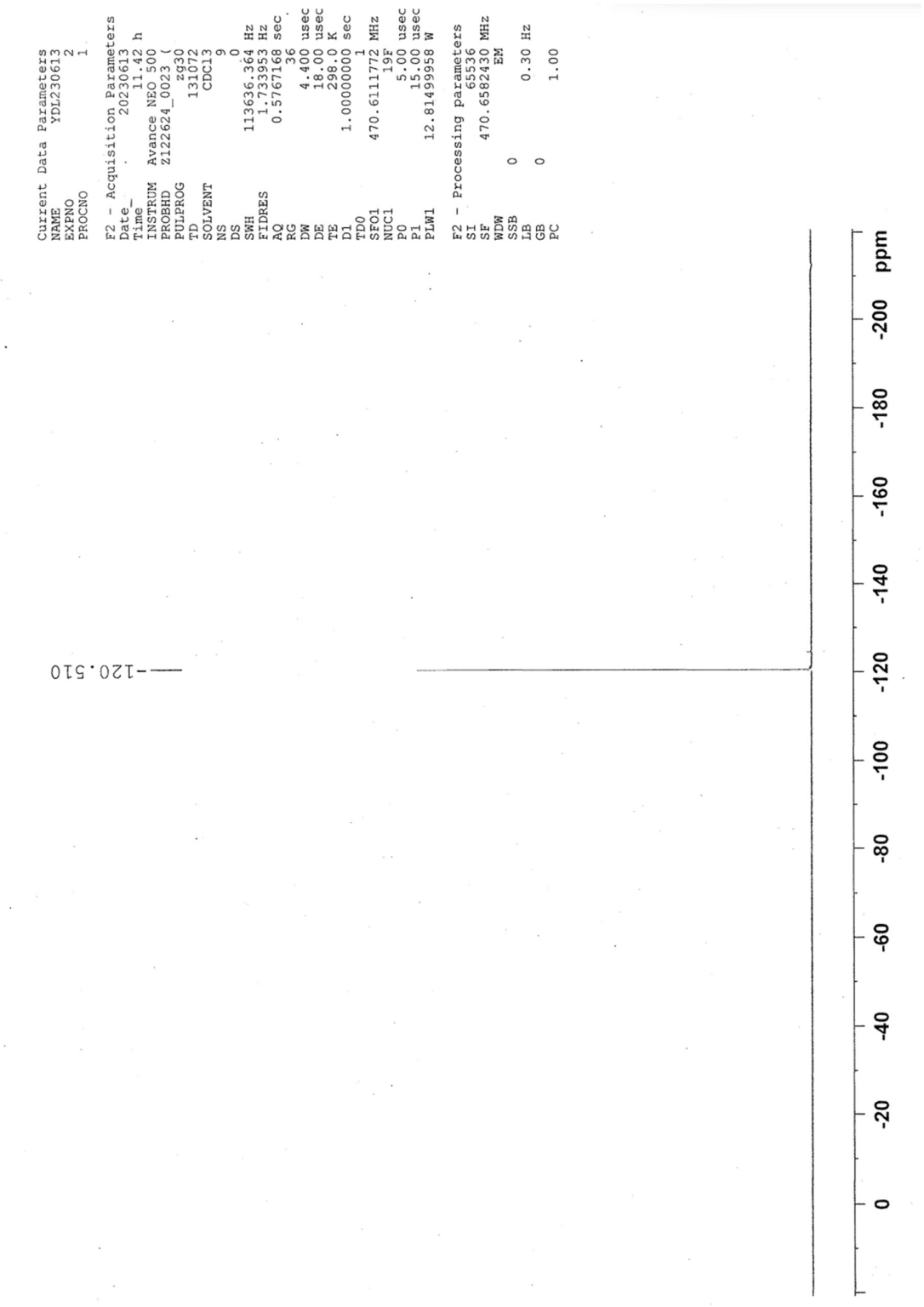

Figure S9. ^{19}F NMR spectrum of compound **YC-H**.

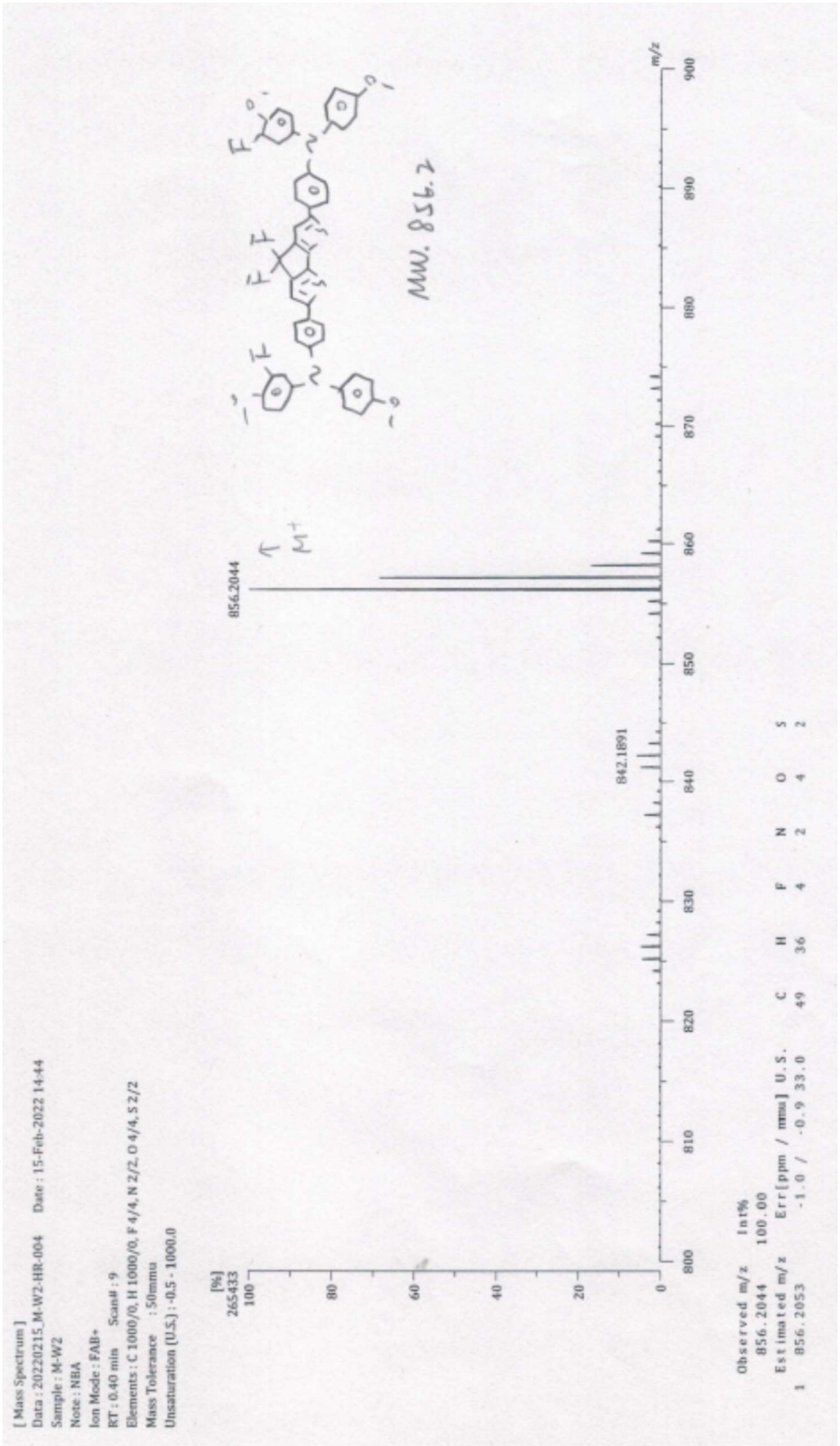

Figure S10. Mass spectra of **YC-oF**.

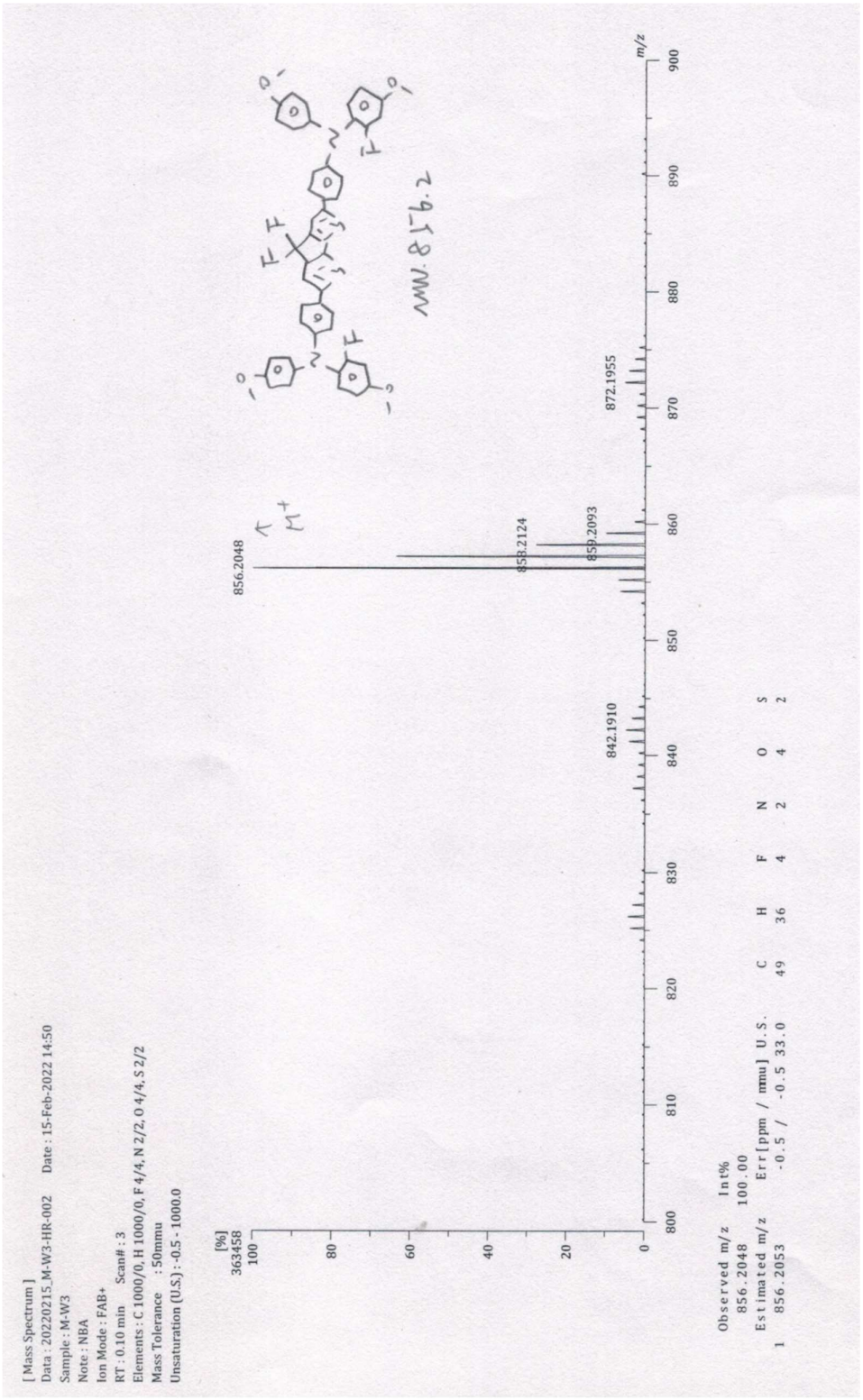

Figure S11. Mass spectra of **YSH-mF**.

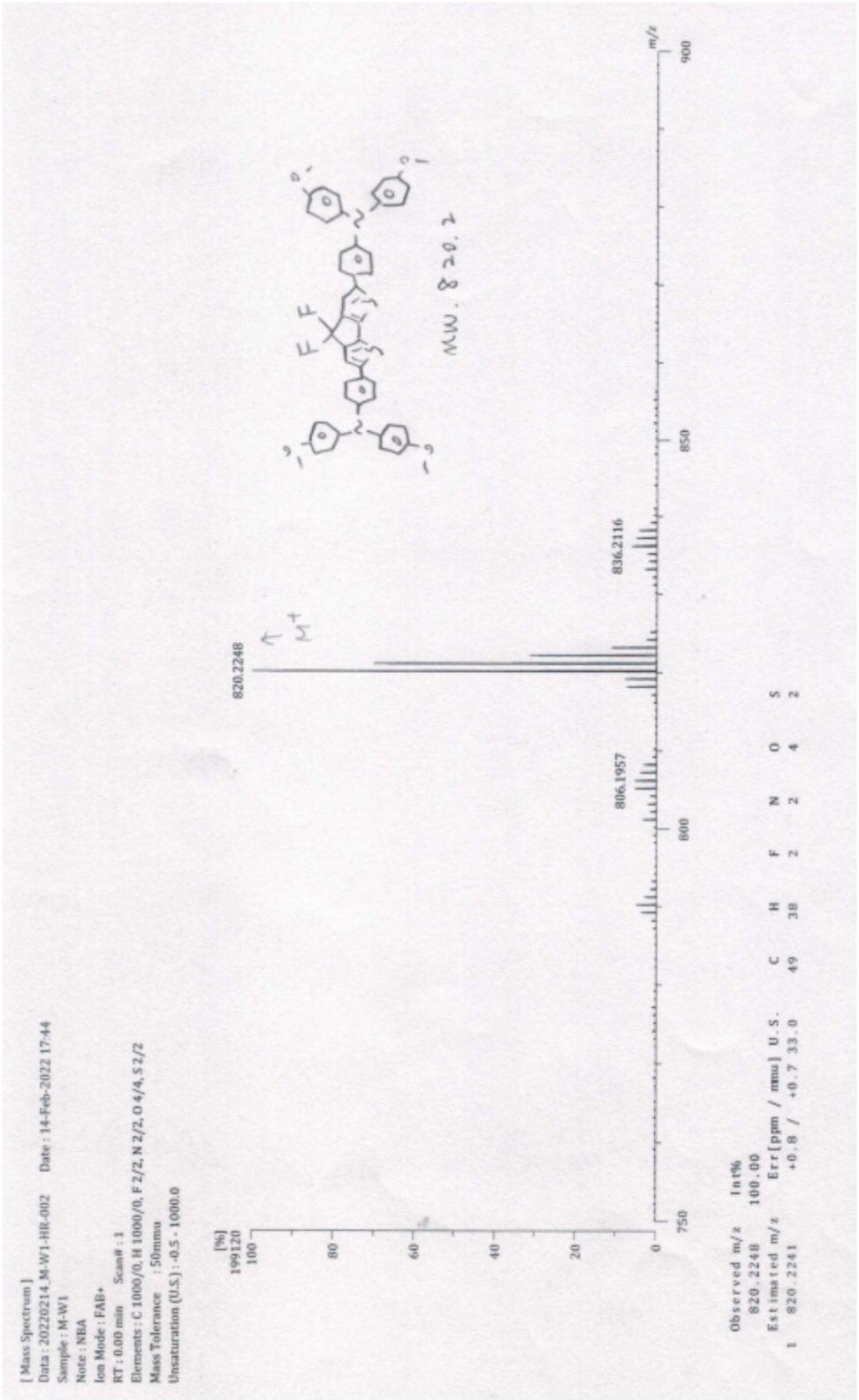

Figure S12. Mass spectra of **YC-H**.

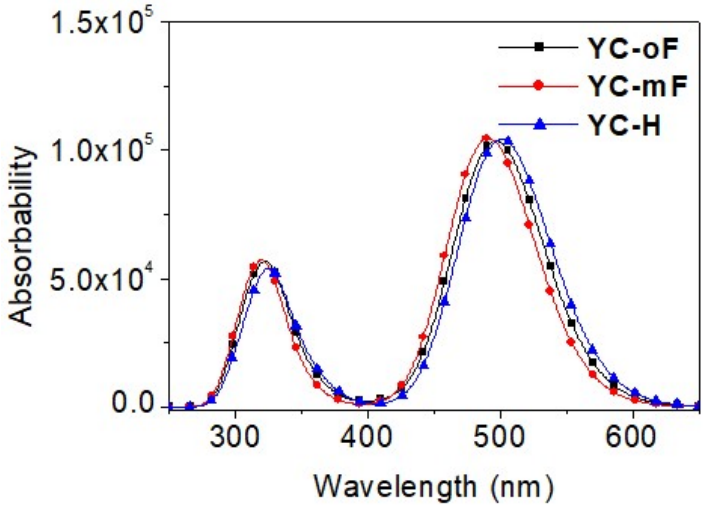

Figure S13. Calculated gas-phase absorption spectra of **YC-oF**, **YC-mF**, and **YC-H**.

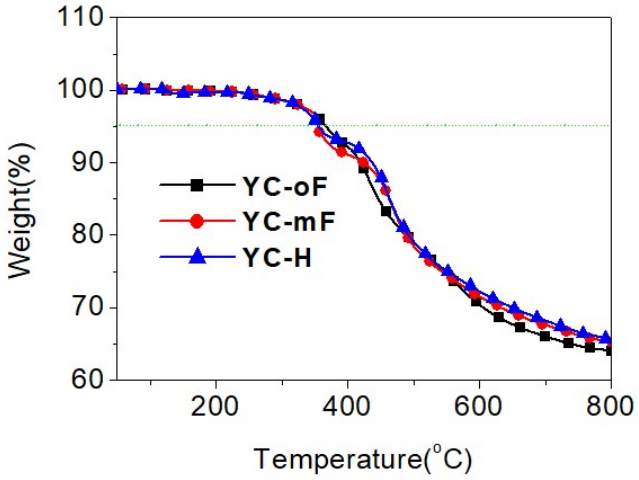

Figure S14. TGA curves of the **YC** series.

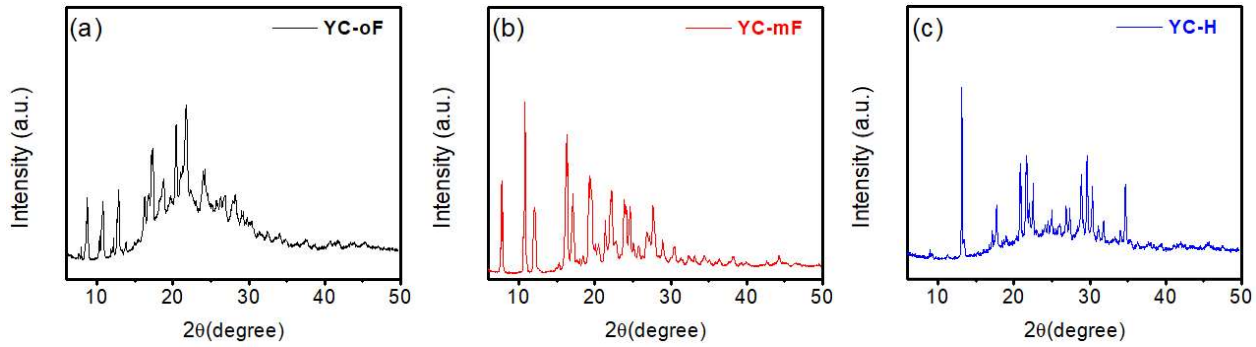

Figure S15. PXRD powder patterns of (a) **YC-oF**, (b) **YC-mF**, and (c) **YC-H**.

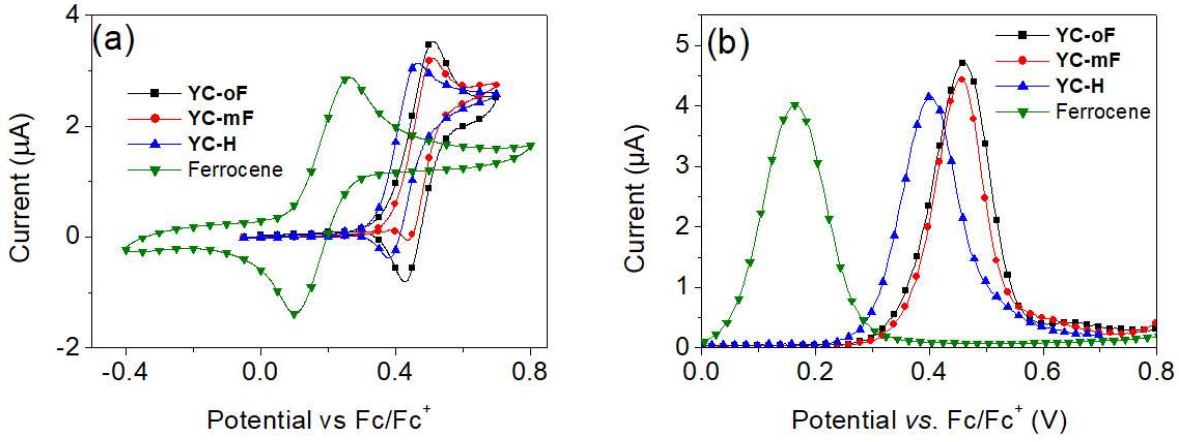

Figure S16. (a) Cyclic voltammetry (CV) and (b) differential pulsed voltammetry (DPV) of **YC** series and ferrocene in THF solution.

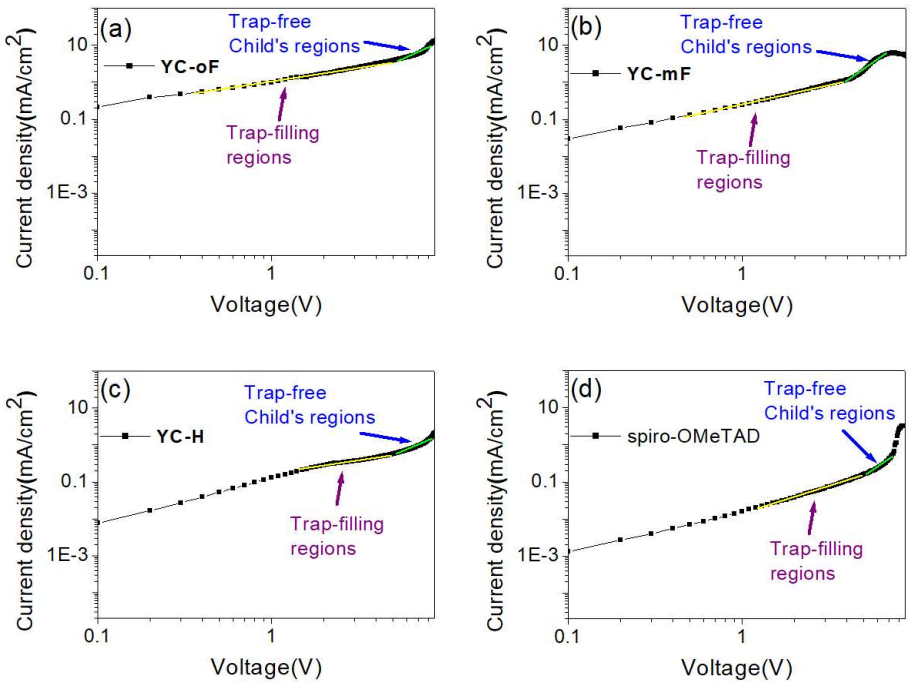

Figure S17. Space-charge-limited-current plots in the *J-V* characteristics of the devices with **YC-oF**, **YC-mF**, **YC-H** and spiro-OMeTAD as HTM, respectively.

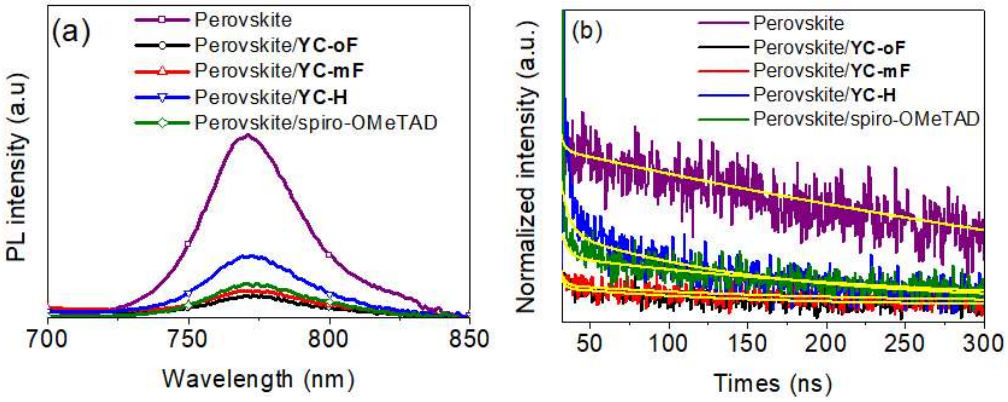

Figure S18. (a) Steady-state photoluminescence spectra and (b) Time-resolved photoluminescence (TRPL) spectra of pristine perovskite and perovskite with HTMs.

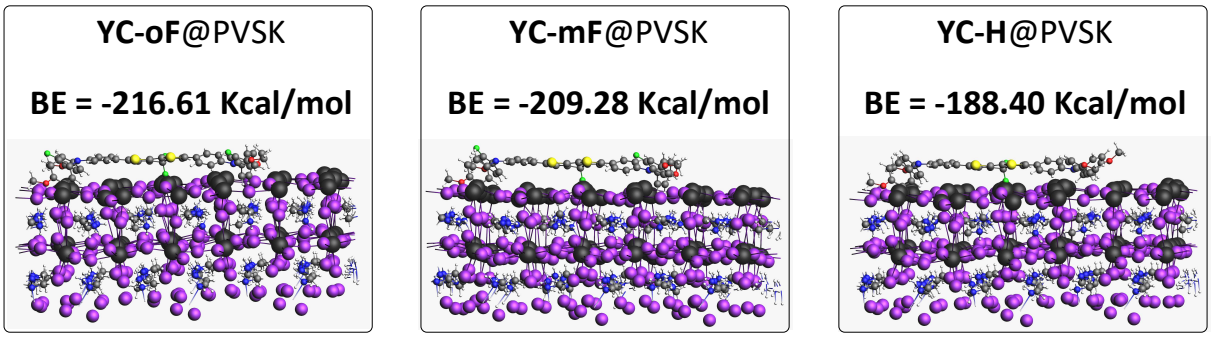

Figure S19. Binding energy of HTMs on the perovskite surface.

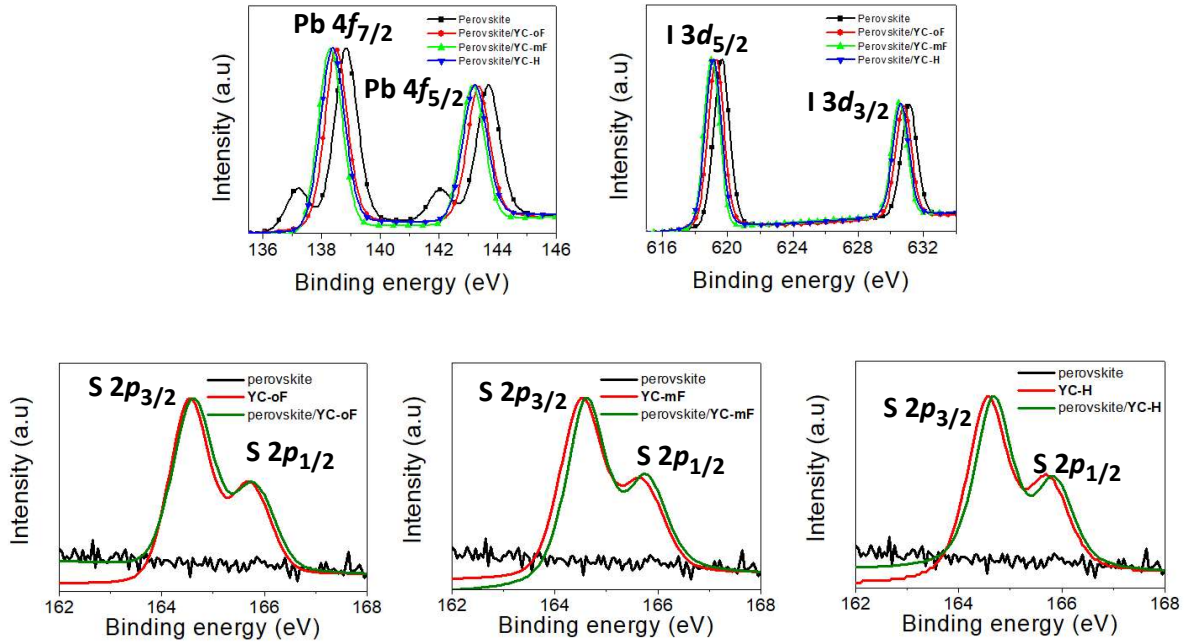

Figure S20. XPS signals of Pb 4*f*, I 3*d*, and S 2*p* from the pristine **YC-oF**, **YC-mF** and **YC-H** film and **YC-oF**, **YC-mF** and **YC-H** coated perovskite film.

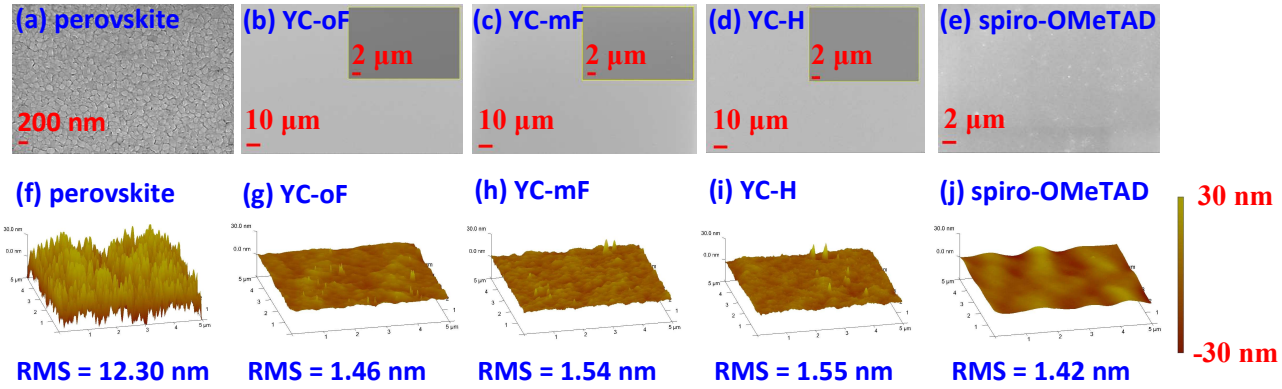

Figure S21. The top-view SEM images (a-e) and AFM three-dimensional surface plots (f-j) of perovskite film and perovskite/HTMs.

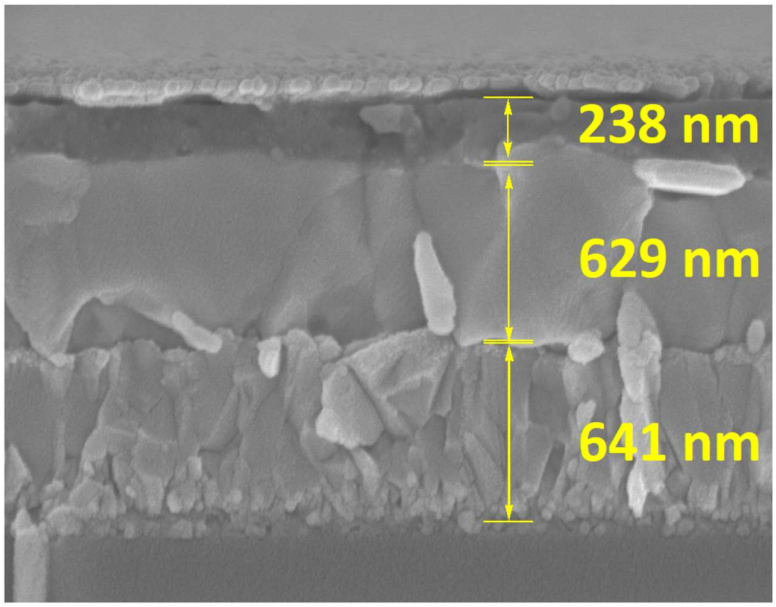

Figure S22. Cross-sectional SEM image of PSCs with the device structure of FTO/SnO_2/perovskite/**YC-oF**/Ag.

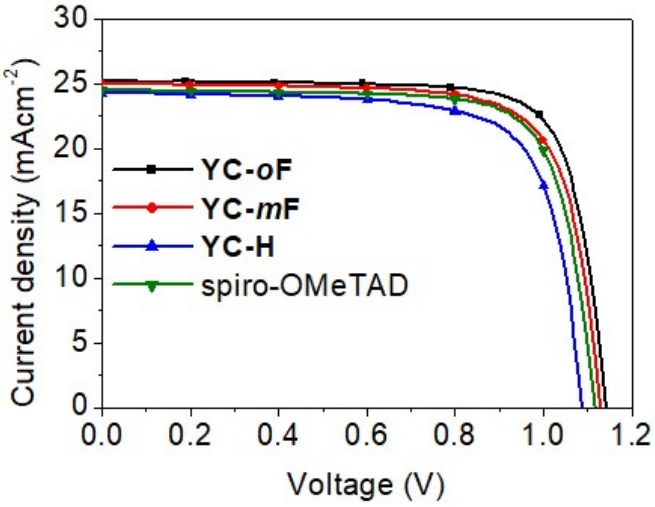

Figure S23. Plots of *J-V* curves for the perovskite solar cells using **YC** series and spiro-OMeTAD as HTM under forward scan (at illumination of 100 mW/cm^2, AM1.5G).

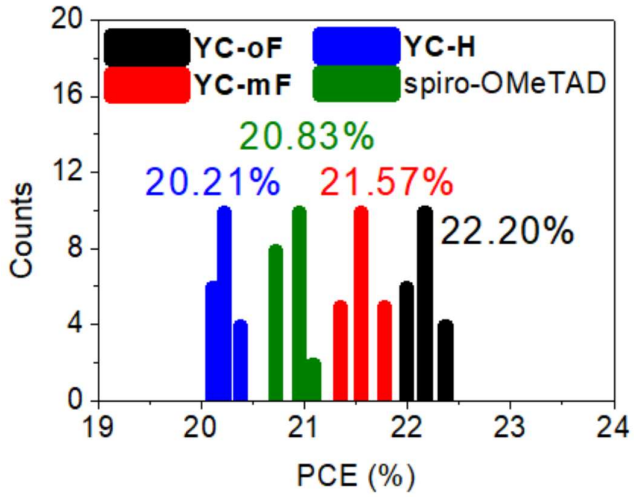

Figure S24. Histogram of PCEs from 20 individual PSCs based on **YC** series and spiro-OMeTAD.

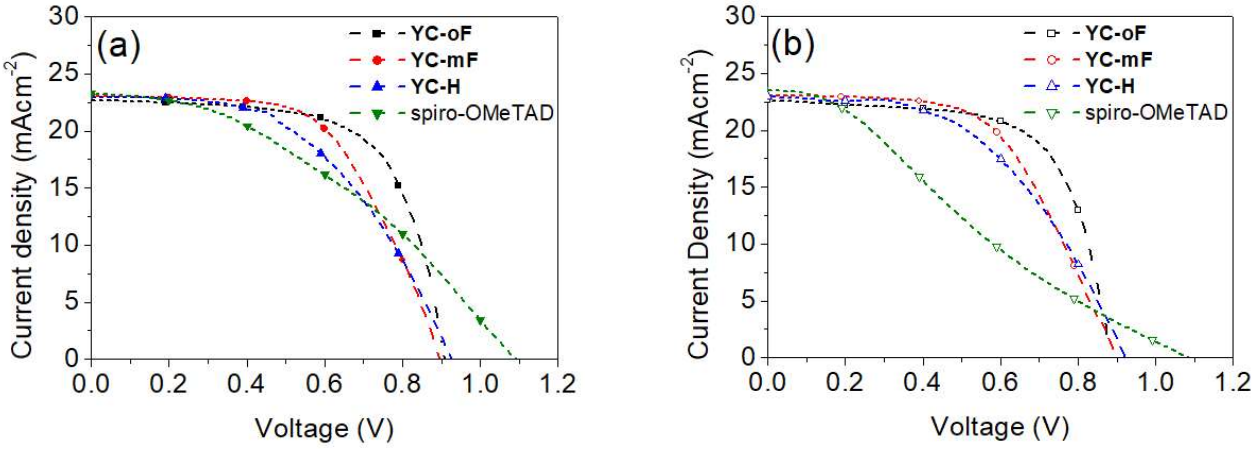

Figure S25. *J-V* curves of the PSCs with different dopant-free HTMs based on **YC** series and spiro-OMeTAD for (a) reverse scan and (b) forward scan.

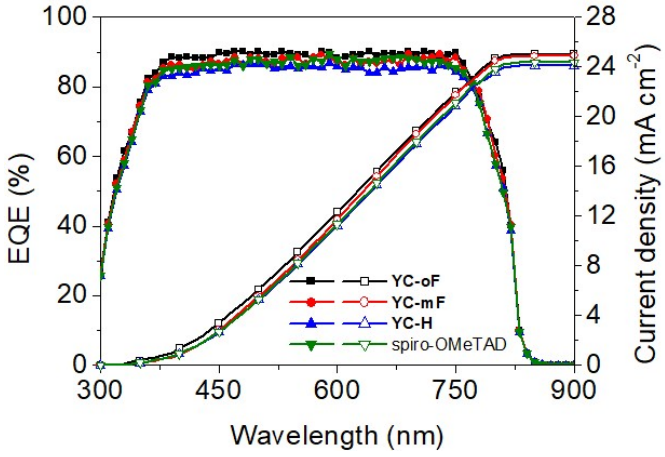

Figure S26. Corresponding IPCE spectra and integrated photocurrent for devices with **YC** series and spiro-OMeTAD.

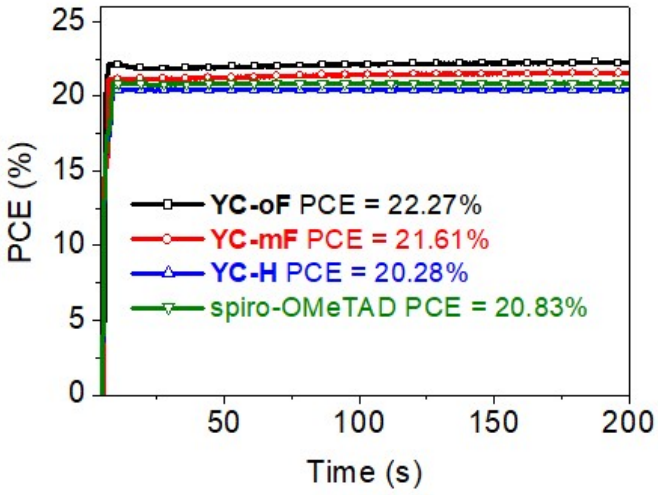

Figure S27. Stabilized power output of PSC devices for **YC** series and Spiro-OMeTAD at their maximum power point.

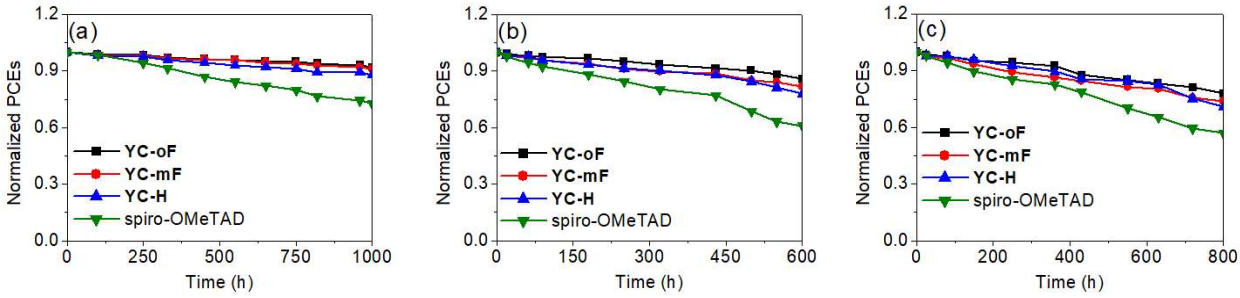

Figure S28. Normalized long-term device stability of **YC-oF**, **YC-mF**, **YC-H** and spiro-OMeTAD-based PSCs: (a) stored at 20-25 °C environment; (b) thermal stressed at 85 °C; and (c) continuous light soaking in glovebox at 40 °C.

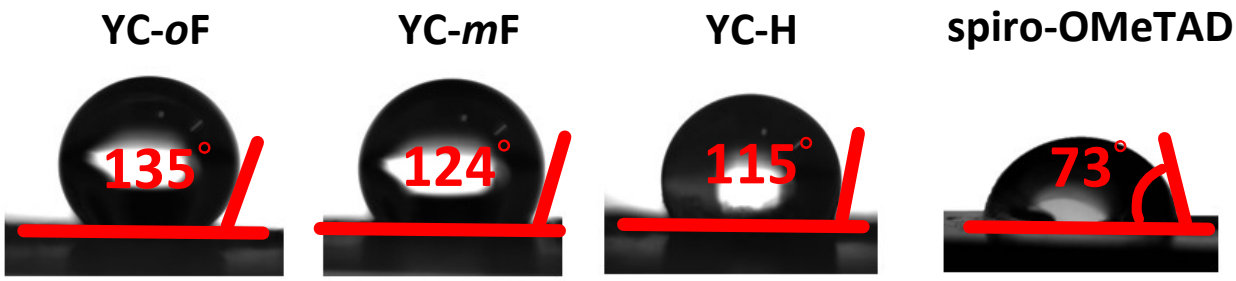

Figure S29. The water contact angles on **YC-oF**, **YC-mF**, **YC-H** and spiro-OMeTAD films.

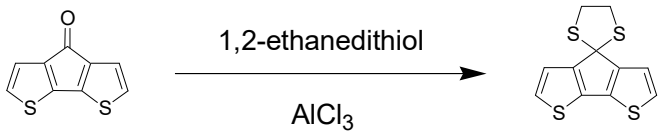

A1

Table S1 Cost Calculation of Compound **A1**

Reagent	**Amount (g)**	**Amount (mL)**	**Price ($/g or $/mL)**	**Total Price ($)**
4H-cyclopenta[2,1-b-3,4-b']dithiophen-4-one	0.11		20	2.2
1,2-ethanedithiol	0.082		0.97	0.08
$AlCl_3$	0.24		0.016	0.003
Dichloromethane		200	0.0149	2.98
Water		150	0	0
Hexane		700	0.0011	0.77
Silica gel	40		0.0042	0.168
Total Cost	6.201$			
Total amount of compound **A1**	0.14 g			
Cost of compound **A1**	44.29 $/g			

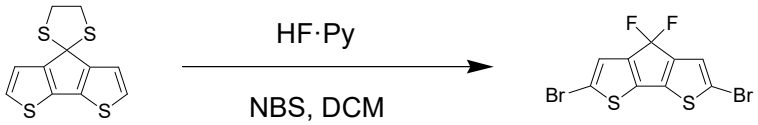

A1 **8**

Table S2 Cost Calculation of Compound **8**

Reagent	**Amount (g)**	**Amount (mL)**	**Price ($/g or $/mL)**	**Total Price ($)**
A1	0.105		44.29	4.65
NBS	0.489		0.094	0.046
HF·Py		1	1.4	1.4
Dichloromethane		4	0.0149	0.0596
Hexane		100	0.0011	0.11
Silica gel	20		0.0042	0.084
Total Cost	6.34$			
Total amount of compound **8**	0.083 g			
Cost of compound **8**	76.39 $/g			

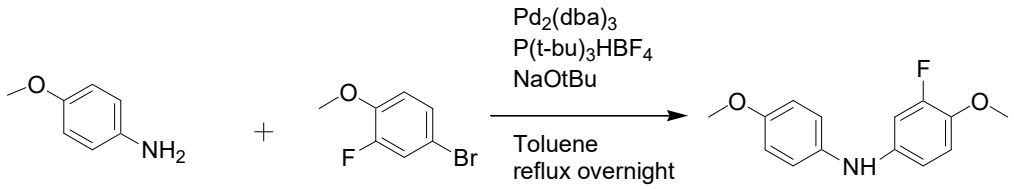

1

Table S3 Cost Calculation of Compound **1**

Reagent	**Amount (g)**	**Amount (mL)**	**Price ($/g or $/mL)**	**Total Price ($)**
p-anisidine	6		0.26	1.56
4-bromo-2-fluoro-1-methoxybenzene	10.494		13.33	139.89
$Pd_2(dba)_3$	0.446		26.16	11.67
$P(t\text{-}bu)_3HBF_4$	0.424		36.33	15.40
sodium tert-butoxide	9.36		0.48	4.49
Toluene		80	0.004	0.32
Dichloromethane		600	0.0149	8.94
Water		150	0	0
Hexane		1400	0.0011	1.54
Silica gel	80		0.0042	0.336
Total Cost	184.146$			
Total amount of compound **1**	10.4 g			
Cost of compound **1**	17.706 $/g			

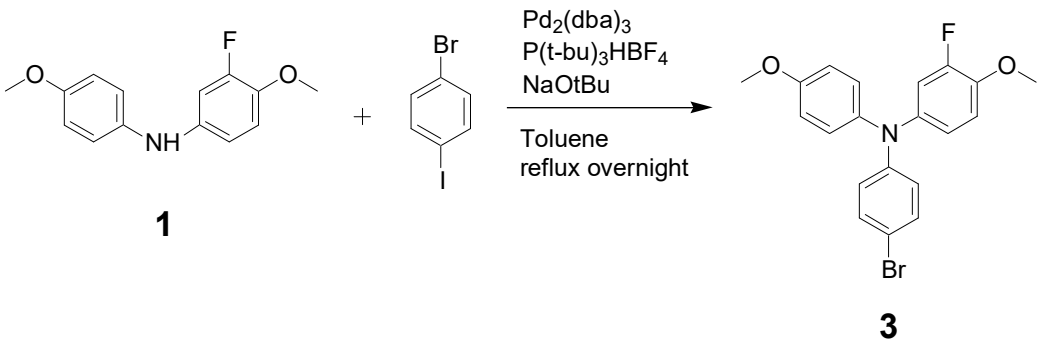

1 **3**

Table S4 Cost Calculation of Compound **3**

Reagent	**Amount (g)**	**Amount (mL)**	**Price ($/g or $/mL)**	**Total Price ($)**
1	6		17.706	106.236
1-Bromo-4-iodobenzene	13.72		8.133	111.598
$Pd_2(dba)_3$	0.448		26.16	11.72
DPPF	0.544		26.666	14.507
sodium tert-butoxide	4.663		0.48	2.24
Toluene		50	0.004	0.2
Dichloromethane		400	0.0149	5.96
Water		150	0	0
Hexane		1200	0.0011	1.32
Silica gel	80		0.0042	0.336
Total Cost	254.117$			
Total amount of compound **3**	8.30 g			
Cost of compound **3**	30.62 $/g			

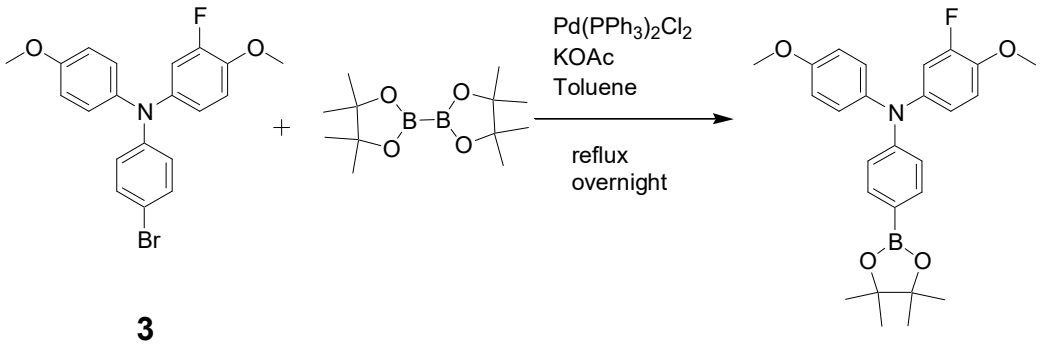

Table S5 Cost Calculation of Compound **5**

Reagent	**Amount (g)**	**Amount (mL)**	**Price ($/g or $/mL)**	**Total Price ($)**
3	5		30.62	153.1
$Pd(PPh_3)_2Cl_2$	0.51		10.71	5.46
Bis(pinacolato)diboron	3.768		0.36	1.356
KOAc	3.85		0.04	0.154
Toluene		125	0.004	0.5
Dichloromethane		800	0.0149	11.92
Water		200	0	0
Hexane		800	0.0011	0.88
Silica gel	80		0.0042	0.336
Total Cost	173.706$			
Total amount of compound **5**	4.75 g			
Cost of compound **5**	36.57 $/g			

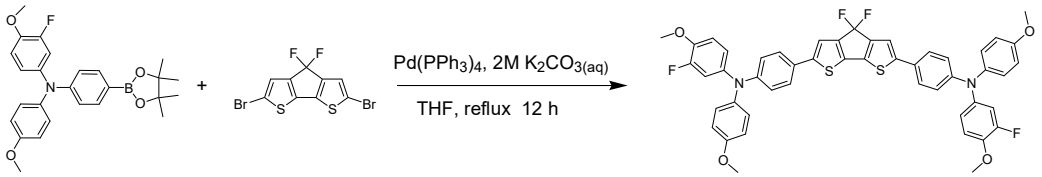

5 **8** **YC-oF**

Table S6 Cost Calculation of Compound **YC-oF**

Reagent	**Amount (g)**	**Amount (mL)**	**Price ($/g or $/mL)**	**Total Price ($)**
8	0.187		76.39	14.28
5	0.5		36.57	18.285
$Pd(PPh_3)_4$	0.036		22.24	0.80
K_2CO_3	0.355		0.03	0.011
Water		50	0.00	0.00
THF		3	0.034	0.102
$MgSO_4$	1		0.06	0.06
Hexane		50	0.0011	0.055
Dichloromethane		150	0.0149	2.235
Silica gel	20		0.0042	0.084
Total Cost	35.912$			
Total amount of **YC-oF**	0.325 g			
Cost of **YC-oF**	110.50 $/g			

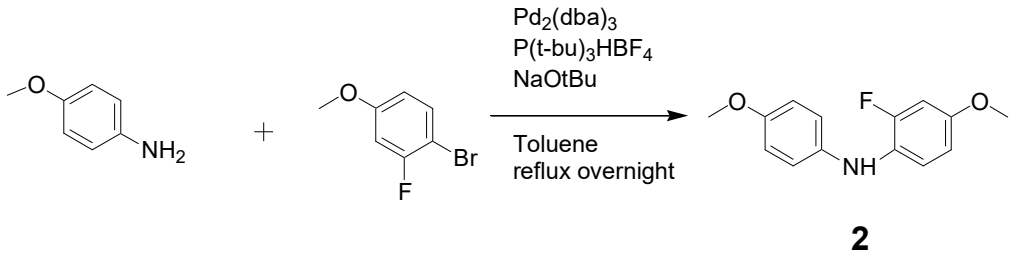

2

Table S7 Cost Calculation of Compound **2**

Reagent	**Amount (g)**	**Amount (mL)**	**Price ($/g or $/mL)**	**Total Price ($)**
p-anisidine	6		0.26	1.56
4-bromo-3-fluoro-1-methoxybenzene	10.56		4.133	43.64
$Pd_2(dba)_3$	0.446		26.16	11.67
$P(t\text{-}bu)_3HBF_4$	0.424		36.33	15.40
sodium tert-butoxide	9.36		0.48	4.49
Toluene		80	0.004	0.32
Dichloromethane		600	0.0149	8.94
Water		150	0	0
Hexane		1400	0.0011	1.54
Silica gel	80		0.0042	0.336
Total Cost	87.896$			
Total amount of compound **2**	9.8 g			
Cost of compound **2**	8.969 $/g			

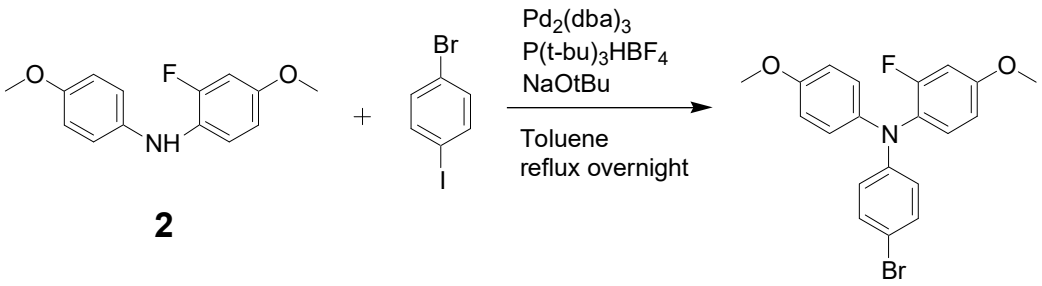

2 **4**

Table S8 Cost Calculation of Compound **4**

Reagent	**Amount (g)**	**Amount (mL)**	**Price ($/g or $/mL)**	**Total Price ($)**
2	6		8.969	53.814
1-Bromo-4-iodobenzene	13.72		8.133	111.598
$Pd_2(dba)_3$	0.448		26.16	11.72
DPPF	0.544		26.666	14.507
sodium tert-butoxide	4.663		0.48	2.24
Toluene		50	0.004	0.2
Dichloromethane		400	0.0149	5.96
Water		150	0	0
Hexane		1200	0.0011	1.32
Silica gel	80		0.0042	0.336
Total Cost	201.695$			
Total amount of compound **4**	8.20 g			
Cost of compound **4**	24.60 $/g			

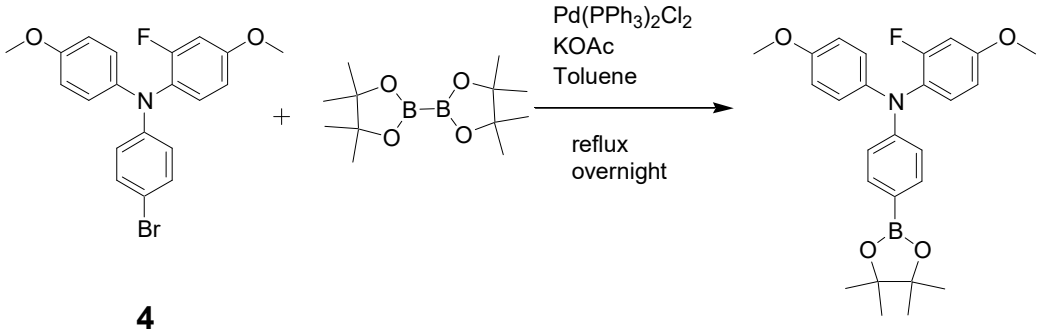

4 **6**

Table S9 Cost Calculation of Compound **6**

Reagent	**Amount (g)**	**Amount (mL)**	**Price ($/g or $/mL)**	**Total Price ($)**
4	5		24.60	122.98
$Pd(PPh_3)_2Cl_2$	0.51		10.71	5.46
Bis(pinacolato)diboron	3.768		0.36	1.356
KOAc	3.85		0.04	0.154
Toluene		125	0.004	0.5
Dichloromethane		800	0.0149	11.92
Water		200	0	0
Hexane		800	0.0011	0.88
Silica gel	80		0.0042	0.336
Total Cost	143.59$			
Total amount of compound **6**	4.08 g			
Cost of compound **6**	35.19 $/g			

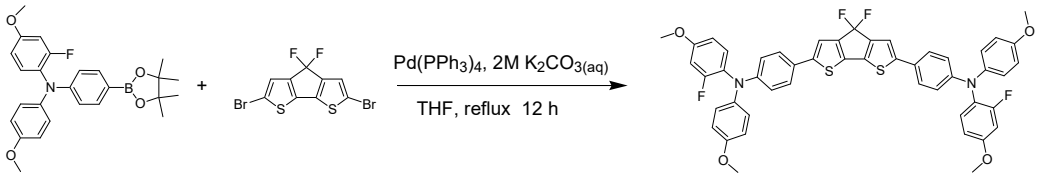

6 **8** **YC-mF**

Table S10 Cost Calculation of Compound **YC-mF**

Reagent	**Amount (g)**	**Amount (mL)**	**Price ($/g or $/mL)**	**Total Price ($)**
8	0.187		76.39	14.28
6	0.5		35.19	17.595
$Pd(PPh_3)_4$	0.036		22.24	0.80
K_2CO_3	0.355		0.03	0.011
Water		50	0.00	0.00
THF		3	0.034	0.102
$MgSO_4$	1		0.06	0.06
Hexane		50	0.0011	0.055
Dichloromethane		150	0.0149	2.235
Silica gel	20		0.0042	0.084
Total Cost	35.222$			
Total amount of **YC-mF**	0.317 g			
Cost of **YC-mF**	111.10 $/g			

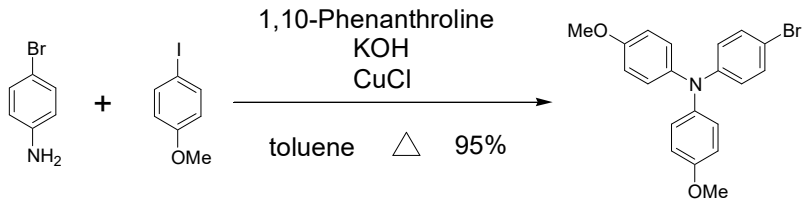

A2

Table S11 Cost Calculation of Compound **A2**

Reagent	**Amount (g)**	**Amount (mL)**	**Price ($/g or $/mL)**	**Total Price ($)**
4-Iodoanisole	2.01		0.18	0.362
4-Bromoaniline	0.49		0.12	0.0588
CuCl	0.01		0.06	0.0006
KOH	1.29		0.02	0.026
1,10-Phenanthroline	0.02		1.04	0.021
Toluene		15	0.004	0.06
Dichloromethane		300	0.0149	4.47
Water		150	0	0
Hexane		700	0.0011	0.77
Silica gel	50		0.0042	0.21
Total Cost	5.978$			
Total amount of compound **A2**	1.04 g			
Cost of compound **A2**	5.748 $/g			

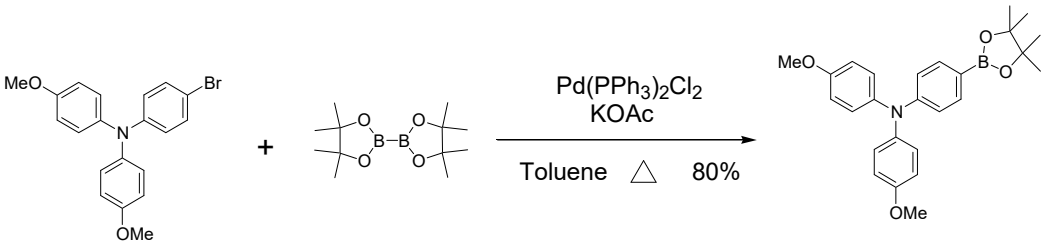

A2 **7**

Table S12 Cost Calculation of Compound **7**

Reagent	**Amount (g)**	**Amount (mL)**	**Price ($/g or $/mL)**	**Total Price ($)**
A2	1.08		5.748	6.66
$Pd(PPh_3)_2Cl_2$	0.06		10.71	0.643
Bis(pinacolato)diboron	0.86		0.36	0.31
KOAc	0.85		0.04	0.81
Toluene		20	0.004	0.08
Dichloromethane		150	0.0149	2.235
Water		200	0	0
Hexane		200	0.0011	0.22
Silica gel	40		0.0042	0.168
Total Cost	11.126$			
Total amount of compound **7**	0.97 g			
Cost of compound **7**	11.47 $/g			

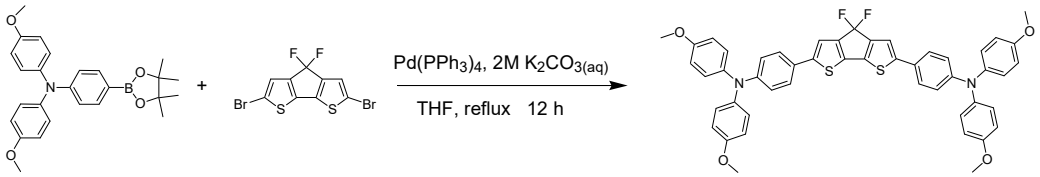

7 **8** **YC-H**

Table S13 Cost Calculation of Compound **YC-H**

Reagent	**Amount (g)**	**Amount (mL)**	**Price ($/g or $/mL)**	**Total Price ($)**
8	0.218		76.39	16.65
7	0.5		11.47	5.735
$Pd(PPh_3)_4$	0.027		22.24	0.60
K_2CO_3	0.355		0.03	0.011
Water		50	0.00	0.00
THF		4	0.034	0.136
$MgSO_4$	1		0.06	0.06
Hexane		50	0.0011	0.055
Dichloromethane		150	0.0149	2.235
Silica gel	20		0.0042	0.084
Total Cost	25.566$			
Total amount of **YC-H**	0.338 g			
Cost of **YC-H**	75.64 $/g			

Table S14 Calculated TDDFT excitation energies (*E*), oscillator strengths (*f*), MO compositions and characters for **YC-oF**.

HTM	n	E(eV, nm)	f	Composition	Character
YC-oF	1	2.4963	1.5353	100% HOMO → LUMO	CT
	2	2.9417	0.0318	100% HOMO-1 → LUMO	π→π*
	3	3.4629	0.1001	100% HOMO-2 → LUMO	π→π*
	4	3.6161	0.0275	15% HOMO-1 → LUMO+3	π→π*
				15% HOMO → LUMO+1	π→π*
				6% HOMO → LUMO+2	π→π*
				64% HOMO → LUMO+3	π→π*
	5	3.6307	0.0226	3% HOMO-1 → LUMO+2	π→π*
				3% HOMO-1 → LUMO+4	π→π*
				73% HOMO → LUMO+1	π→π*
				3% HOMO → LUMO+2	π→π*
				18% HOMO → LUMO+3	π→π*
	6	3.6595	0.0117	26% HOMO-1 → LUMO+2	π→π*
				10% HOMO → LUMO+1	π→π*
				64% HOMO → LUMO+2	π→π*

Table S15 Calculated TDDFT excitation energies (*E*), oscillator strengths (*f*), MO compositions and characters for **YC-mF**.

HTM	n	E(eV, nm)	f	Composition	Character
YC-mF	1	2.5248	1.5506	100% HOMO → LUMO	CT
	2	3.0045	0.0107	100% HOMO-1 → LUMO	π→π*
	3	3.5194	0.0691	100% HOMO-2 → LUMO	π→π*
	4	3.5812	0.0299	4% HOMO-1 → LUMO+1	π→π*
				16% HOMO → LUMO+2	π→π*
				23% HOMO → LUMO+1	π→π*
				57% HOMO → LUMO+2	π→π*
	5	3.6225	0.0106	19% HOMO-1 → LUMO+3	π→π*
				10% HOMO → LUMO+1	π→π*
				10% HOMO → LUMO+2	π→π*
				61% HOMO → LUMO+3	π→π*
	6	3.7121	0.0274	3% HOMO-1 → LUMO+4	π→π*
				62% HOMO → LUMO+1	π→π*
				16% HOMO → LUMO+2	π→π*
				19% HOMO → LUMO+3	π→π*

Table S16 Calculated TDDFT excitation energies (*E*), oscillator strengths (*f*), MO compositions and characters for **YC-H**.

HTM	n	E(eV, nm)	f	Composition	Character
YC-H	1	2.4733	1.5461	100% HOMO → LUMO	CT
	2	2.9102	0.0112	100% HOMO-1 → LUMO	π→π*
	3	3.4549	0.1124	100% HOMO-2 → LUMO	π→π*
	4	3.5435	0.0352	8% HOMO-1 → LUMO+2	π→π*
				14% HOMO-1 → LUMO+3	π→π*
				64% HOMO → LUMO+2	π→π*
				14% HOMO → LUMO+3	π→π*
	5	3.559	0.0082	16% HOMO-1 → LUMO+2	π→π*
				8% HOMO-1 → LUMO+3	π→π*
				14% HOMO → LUMO+2	π→π*
				62% HOMO → LUMO+3	π→π*
	6	3.6394	0.0329	3% HOMO-1 → LUMO+4	π→π*
				97% HOMO → LUMO+1	π→π*

Table S17. Summary of the fitting results and corresponding dynamic parameters derived from TRPL decay traces.

HTM	A_1 (%)	τ_1 (ns)	A_2 (%)	τ_2 (ns)	$\tau_{avg.}$ (ns)
Pristine perovskite	85	2.26	15	647.30	104.89
YC-oF	93	1.94	7	114.97	9.91
YC-mF	88	2.1	12	117.10	15.89
YC-H	83	2.33	17	197.3	35.47
Spiro-OMeTAD	74	4.72	26	115.44	33.51

Table S18 Summary of photovoltaic characteristics extracted from *J-V* curves of perovskite solar cells without dopant under different scan direction

HTM	scan direction	V_{oc}/V	J_{sc}/mA cm^{-2}	FF (%)	PCE(%)
YC-*o*F	reverse	0.907	22.69	65.61	13.48
	forward	0.884	22.64	66.05	13.20
YC-*m*F	reverse	0.896	23.11	58.66	12.12
	forward	0.897	23.08	56.44	11.67
YC-H	reverse	0.927	22.96	50.03	10.63
	forward	0.921	22.95	49.68	10.49
spiro-OMeTAD	reverse	1.09	23.27	38.43	9.75
	forward	1.09	23.52	24.54	6.29

Table S19 Photophysical and electrochemical data of **YC-oF**, **YC-mF**, and **YC-H**

HTM	λ_{abs} (nm) ($\varepsilon\times 10^{-4}$/M^{-1} cm^{-1}) [a]	λ_f (nm) [a]	E_{HOMO} (eV) [b]	$E_{0\text{-}0}$ (eV) [c]	E_{LUMO} (eV) [d]	E_{HOMO} (eV) [e]	$E_{0\text{-}0}$ (eV) [e]	E_{LUMO} (eV) [e]	T_d (°C) [f]
YC-oF	463 (4.7)	558	-5.40	2.37	-3.03	-4.52	2.75	-1.77	368
YC-mF	459 (5.3)	555	-5.38	2.38	-3.00	-4.46	2.77	-1.69	348
YC-H	468 (4.5)	564	-5.33	2.34	-2.99	-4.41	2.75	-1.66	357

[a] Maxima of the absorption and fluorescence band in THF solution; [b] Determined from the differential pulse voltammetry; [c] The value of $E_{0\text{-}0}$ was obtained from the intersection of normalized absorption and photoluminescence spectra; [d] Energy of the LUMO of the compounds estimated by $E_{HOMO}+E_{0\text{-}0;}$ [e] TDDFT/B3LYP/6-31G(d,p) level calculated values. [f] Decomposition temperatures (T_d) observed from TGA.

References

[1] K.-M. Lee, Y.-H. Huang, W.-H. Chiu, Y.-K. Huang, G. Chen, G. B. Adugna, S.-R. Li, F. J. Lin, S.-I. Lu, H. C. Hsieh, K.-L, Liau, C.-C. Huang, Y. Tai, Y. T. Tao, Y.-d. Lin, Adv. Funct. Mater. 2023, 2306367.

[2] Y. Le, M. Nitani, M. Ishikawa, K.-I. Nakayama, H. Tada, T. Kaneda, Y. Aso, Org. Lett. 2007, 9, 2115-2118.

[3] H. R. Tseng, H. Phan, C. Luo, M. Wang, L. A. Perez, S. N. Patel, L. Ying, E. J. Kramer, T. Q. Nguyen, G. C. Bazan, A. J. Heeger, Adv. Mater. 2014, 26, 2993−2998.

[4] A. Austin, G. A. Petersson, M. J. Frisch, F. J. Dobek, G. Scalmani, K. Throssell, J. Chem. Theory Comput., 2012, 8, 4989-5007.

[5] Gaussian 16, Revision A.03, M. J. Frisch, G. W. Trucks, H. B. Schlegel, G. E. Scuseria, M. A. Robb, J. R. Cheeseman, G. Scalmani, V. Barone, G. A. Petersson, H. Nakatsuji, X. Li, M. Caricato, A. V. Marenich, J. Bloino, B. G. Janesko, R. Gomperts, B. Mennucci, H. P. Hratchian, J. V. Ortiz, A. F. Izmaylov, J. L. Sonnenberg, D. Williams-Young, F. Ding, F. Lipparini, F. Egidi, J. Goings, B. Peng, A. Petrone, T. Henderson, D. Ranasinghe, V. G. Zakrzewski, J. Gao, N. Rega, G. Zheng, W. Liang, M. Hada, M. Ehara, K. Toyota, R. Fukuda, J. Hasegawa, M. Ishida, T. Nakajima, Y. Honda, O. Kitao, H. Nakai, T. Vreven, K. Throssell, J. A. Montgomery, Jr., J. E. Peralta, F. Ogliaro, M. J. Bearpark, J. J. Heyd, E. N. Brothers, K. N. Kudin, V. N. Staroverov, T. A. Keith, R. Kobayashi, J. Normand, K. Raghavachari, A. P. Rendell, J. C. Burant, S. S. Iyengar, J. Tomasi, M. Cossi, J. M. Millam, M. Klene, C. Adamo, R. Cammi, J. W. Ochterski, R. L. Martin, K. Morokuma, O. Farkas, J. B. Foresman, and D. J. Fox, Gaussian, Inc., Wallingford CT, 2016.

[6] J. Tomasi, B. Mennucci, R. Cammi, Chem. Rev. 2005, 105, 2999-3093.

[7] S. Grimme, C. Bannwarth, P. Shushkov, A Robust and Accurate Tight-Binding Quantum Chemical Method for Structures, Vibrational Frequencies, and Noncovalent Interactions of Large Molecular Systems Parametrized for All spd-Block Elements (Z = 1-86), J. Chem. Theory Comput., 2017, 13 (5), pp 1989–2009

[8] AMS DFTB 2022.1, SCM, Theoretical Chemistry, Vrije Universiteit, Amsterdam, The Netherlands, http://www.scm.com. Optionally, you may add the following list of authors and contributors: R. Rüger, A. Yakovlev, P. Philipsen, S. Borini, P. Melix, A.F. Oliveira, M. Franchini, T. van Vuren, T. Soini, M. de Reus, M. Ghorbani Asl, T. Q. Teodoro, D. McCormack, S. Patchkovskii, T. Heine.

[9] AMS 2022.1, SCM, Theoretical Chemistry, Vrije Universiteit, Amsterdam, The Netherlands, http://www.scm.com.